Geosystems and Geoenvironment 1 (2022) 1–26

Contents lists available at ScienceDirect

Geosystems and Geoenvironment

journal homepage: www.elsevier.com/locate/geogeo

Mineral systems: Their advantages in terms of developing holistic genetic models and for target generation in global mineral exploration

David I. Groves[a,b], M. Santosh[b,c,d,*], Daniel Müller[e], Liang Zhang[b], Jun Deng[b], Li-Qiang Yang[b], Qing-Fei Wang[b]

[a] Centre for Exploration Targeting, University of Western Australia, Crawley, WA 6009, Australia
[b] State Key Laboratory of Geological Processes and Mineral Resources, China University of Geosciences, 29# Xue-Yuan Road, Haidian District, Beijing 100083, China
[c] Department of Earth Sciences, University of Adelaide, Adelaide, SA 5005, Australia
[d] Division of Interdisciplinary Science, Faculty of Science, Kochi University, Kochi 780-8520, Japan
[e] Consulting Geologist, Las Condes, Santiago, Chile

ARTICLE INFO

Article history:
Received 6 August 2021
Revised 15 August 2021
Accepted 15 August 2021

Keywords:
Mineral systems
Orogenic gold systems
Porphyry Cu-Au systems
Craton margins
Metallogenic factories

ABSTRACT

Since the concept of mineral systems was first proposed, there have been growing calls for their use in deriving holistic genetic models and in assisting in exploration targeting in a world of diminishing mineral discoveries. This is because the mineral systems approach provides a means of integrating information over a range of time and terrane scales using the broad critical components of Geodynamics, Fertility, Architecture, and Preservation. Although their adoption is limited, the value of such mineral systems for single deposit classes and closely related deposit groups is demonstrated and numerous disparate deposit classes are shown to occupy equivalent tectonic niches in terms of their Geodynamic and Preservation components.

The value of a mineral system model for a single deposit class is demonstrated for orogenic gold deposits using the premise that their genesis is explained in terms of a single global model rather than a series of disparate local models. If all orogenic gold deposits define a coherent mineral system, there are only two realistic sources of auriferous fluid, based on their syn-mineralization geodynamic settings. These are from devolatilization of a subducted oceanic slab with its overlying sulfide-rich sedimentary package, or release from mantle lithosphere that was metasomatized and fertilized during a previous subduction event, particularly adjacent to craton margins. This orogenic gold mineral system can be applied to conceptual exploration by first identifying the required settings at Geodynamic to deposit scales. Within these settings, it is then possible to define the critical gold mineralization processes in the system: Fertility, Architecture, and Preservation. These among other parameters, dictate that the structures controlling ore fluid advection must be lithosphere-scale faults that can be identified in magneto-telluric surveys, and that amphibolite-facies metamorphic domains are prospective exploration search spaces.

The porphyry-high sulfidation-skarn Cu-Au (Mo, W, Ag) deposit group is an example where the mineral system comprises several deposit classes that are commonly spatially and temporally associated. These occur in strike extensive, curvilinear volcanic, continental, island, and post-collisional arcs, where Geodynamics and province-scale Architecture are controlled by arc-parallel continental-scale faults and intersections of oblique crustal-scale accommodation structures, commonly in shallow subduction slab arc segments. Fertility of the arcs is indicated by geochemistry of volcanic components that reflect residence and replenishment of H_2O-rich hybrid source magmas in upper crustal magma chambers. In terms of district-scale Architecture, the porphyry-related systems are sited within and above small finger-shaped porphyritic bodies that intrude the roof zones of oxidized granitic plutons. The mineral systems comprise vertically and laterally zoned orebodies, alteration envelopes, and metal ratios developed from long-lived, originally high salinity and low pH, evolving magmatic-hydrothermal fluids exsolved from the fertile porphyry intrusions. Preservation potential is limited because of high uplift and erosion rates in the host arcs, with most deposits restricted to the Cenozoic, although there are Mesozoic examples in

* Corresponding author at: State Key Laboratory of Geological Processes and Mineral Resources, China University of Geosciences, 29# Xue-Yuan Road, Haidian District, Beijing 100083, China.
E-mail address: santosh@cugb.edu.cn (M. Santosh).

https://doi.org/10.1016/j.geogeo.2021.09.001

post-collisional arcs. At district scale, the presence of lithocaps identifies systems at a suitable exhumation level for exploration, with a range of mapping, remote sensing spectral, and geophysical methodologies applicable to detect critical responses from extensive porphyry-related footprints.

Craton and thick lithosphere margins represent Geodynamic settings with high Preservation factors for an incredibly large range of deposit classes enriched in Ag, Au, Bi, Co, Cu, Fe, Mo, Ni, P, Pb, PGE, REE, Sb, Sn, Te, W, and Zn, and including diamonds. These are sited within ~100 km of the margins due to adjacent metasomatized and fertilized mantle lithosphere, development of lithosphere-scale fault arrays, or fertile marginal basins on these margins. Thus, although Fertility and Architecture components vary widely between component mineral systems, the combined Geodynamic and Preservation factors provide specific restricted exploration search spaces for a variety of deposit classes. This is shown in spectacular fashion for the North China and Yangtze cratons in eastern China where 66 diverse giant or world class deposits are sited within ~100 km of their margins.

Contents

1. Introduction

Greenfield mineral exploration is currently an inefficient process with ore deposit discovery rates slowing significantly in the 21st Century (Schodde, 2017) despite increased exploration expenditure. There needs to be a step improvement in greenfield exploration to replenish depleted resources and maintain long-term production. It is evident that conceptual geological targeting is required as an initial step to focus exploration into the most prospective districts within potentially well-endowed terranes or provinces (Hronsky and Groves, 2008). As a crucial first step, this requires the establishment of superior predictive geological models for the deposit type that is sought by the greenfield exploration program.

Research into genetic models for mineralization systems has gradually evolved towards holistic mineral system models that view the mineralization processes in a hierarchical manner from geodynamic setting through province- and district- to deposit-scale. This mineral systems concept was initiated by Wyborn et al. (1994) and championed by Knox-Robinson and Wyborn (1997) and Hronsky and Groves (2008), but it is only since 2010 that it has become prominent as a critical tool for development of genetic models and for conceptual targeting

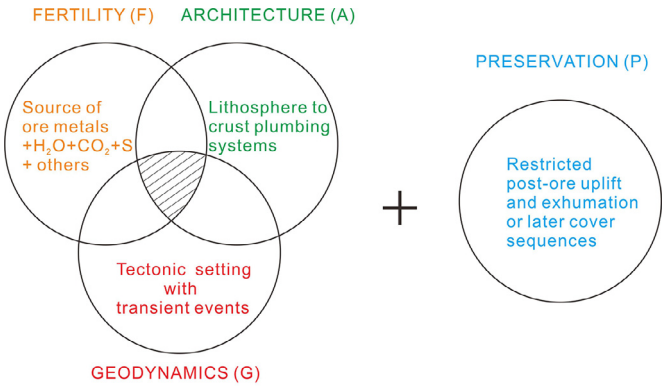

Fig. 1. Critical elements of a mineral system, with emphasis on orogenic gold. Adapted from McCuaig and Hronsky (2014).

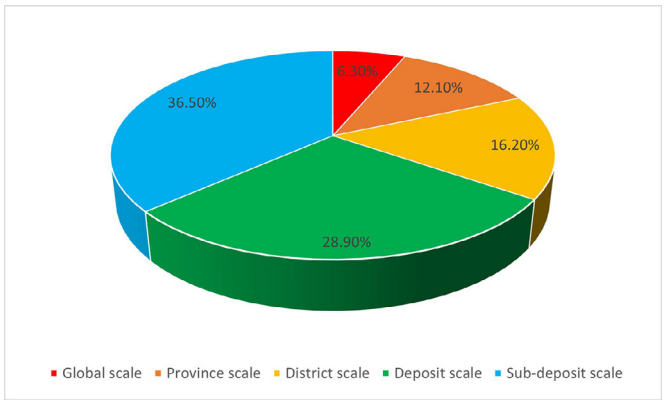

Fig. 2. Pie diagram plot showing percentage of 395 papers published by *Economic Geology* and *Mineralium Deposita* in 2020 and *Ore Geology Reviews* in January to June 2020 (reduced due to larger numbers of papers per issue). Categories defined by subjective selection by first author. Global represents global deposit discussions or methods that can be applied globally. Province (25% of these papers concern geochronology), District, and Deposit represent content at those scales. Sub-deposit represents detailed analytical techniques applied to specific deposits or, less commonly, deposit clusters. An estimated 15% of papers mention exploration in their titles or are adjudged to have exploration significance. Mineral system is in the titles of 0.75% papers.

(Deng et al., 2020a; Groves et al., 2020a; Hagemann et al., 2016; Huston et al., 2016; McCuaig and Hronsky, 2014; McCuaig et al., 2010; Wyman et al., 2016) that has been applied to mineral potential analysis for a variety of mineral commodities (Bruce et al., 2020; McCafferty et al., 2019; Skirrow et al., 2019). As summarized by Kelley et al. (2021), mineral systems models require a Fertile ore-component source in a suitable Geodynamic setting with favourable linked lithosphere and crustal Architecture for ore-fluid migration to a trap site, with suitable post-mineralization tectonic processes to ensure Preservation. It is the multiplication effect of the conjunction of self-organised critical components (Hronsky, 2011, 2020) of the mineral system (Fig. 1) that determines the size and economic value of an ore body (Megill, 1988).

Despite this increasing emphasis on mineral systems rather than the genesis of individual deposits, published economic geology research (Fig. 2) still favours deposit or smaller-scale studies that are heavily weighted towards the application of analytical techniques. The majority of such research produces complex genetic models at the microscale that are inappropriately applied to the deposit or district scale and have little application to global mineral exploration. In this paper, the mineral systems approach

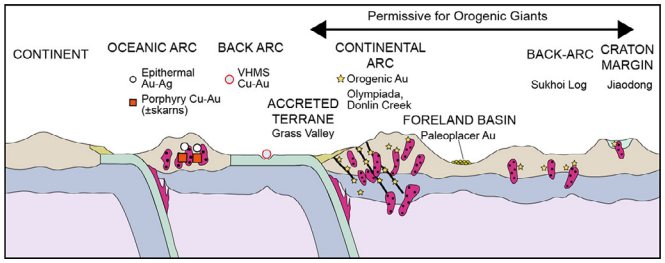

Fig. 3. Convergent margin-orogenic gold model showing range of tectonic settings for orogenic gold systems within a consistent Geodynamic environment. Adapted from Goldfarb et al. (2001), 2005) and Groves et al. (2005a) from initial figure in Groves et al. (1998).

is applied to orogenic gold deposits as a single deposit class, and porphyry-high sulfidation-skarn systems as an example of multi-deposit classes, with deposits sited adjacent to craton margins as an example of the power of grouping diverse deposit classes based on their Geodynamic and related Preservation components. The benefit of applying such a mineral systems approach to exploration targeting is emphasized.

2. A universal genetic model for orogenic gold deposits

2.1. Introduction

Following the pioneering deposit integration studies of Colvine et al. (1984) and Groves (1993), the term orogenic gold deposit was defined by Groves et al. (1998), following Gebre-Mariam et al. (1995), as a coherent group (Fig. 3) of structurally controlled (Kerrich, 1989) gold-only deposits that formed in convergent margin settings (Groves et al., 2005a) in broad thermal equilibrium with their wall-rocks from low-salinity H_2O–CO_2 ore fluids at crustal depths ranging from 2 to 20 km (Groves, 1993; Kolb and Meyer, 2002; Kolb et al., 2005a, 2015b, 2015). Although this term is widely accepted (Bierlein et al., 2006a; Goldfarb et al., 2001, 2005, 2014), there have been numerous models (Groves et al., 2020b: their Fig. 2) to explain the genesis of this deposit group, as summarized by Goldfarb and Groves (2015), which can only be resolved if a mineral systems approach is adopted (Groves et al., 2020b; Wyman et al., 2016).

Goldfarb and Groves (2015), Wyman et al. (2016), and Groves et al. (2020b) present abundant evidence to show that shallow crustal and magmatic-hydrothermal models are not viable for most individual orogenic gold deposits, let alone a single integrated mineral system that incorporates all deposits within the deposit class. This leaves metamorphic models as the only viable universal or near-universal models for the genesis of orogenic gold deposits.

2.2. Search for a holistic genetic model

Since the 1980s, there has been general acceptance of an auriferous fluid source model that promotes metamorphic devolatilization of largely supracrustal rocks within the continental mid-crust under upper greenschist- to amphibolite-facies conditions. Dominant upwards advection of resultant metamorphic low-salinity H_2O–CO_2 (+/- CH_4, N_2) fluid and metals along complex continental fluid pathways (Ridley and Diamond, 2000) to the depositional site of orogenic gold mineralization at higher crustal levels is advocated in this model (summarized by Goldfarb et al., 2005; Phillips and Powell, 2010; Tomkins, 2010; among many others). Deposition of gold in convergent margins occurred consistently during a late transition in deformation from compression to transpression (Groves et al., 2000), more rarely trans-tension, most

commonly during accretion (Goldfarb et al., 1988), with concomitant uplift and lowering of lithostatic pressure (Groves et al., 1987; White et al., 2015).

This crustal metamorphic model has the potential to explain those deposits in mesozonal to epizonal orogenic gold deposits in the terminology of Gebre-Mariam et al. (1995), where peak greenschist-facies metamorphic conditions broadly coincide with the timing of gold mineralization. However, it has significant weaknesses as a universal model. For example, gold-rich fluids would need to have been derived from different volcanic and sedimentary source rocks at different times in Earth history (Goldfarb and Groves, 2015) within different geodynamic settings where anomalous heat flow and consequent regional metamorphism was caused by a variety of crustal- to mantle-related processes (Goldfarb et al., 2005).

There are several weaknesses for the crustal metamorphic model, most obviously for Precambrian deposits, but also for an increasing number of Phanerozoic deposits, particularly in China. These are outlined in detail by Wyman et al. (2016) and Groves et al. (2020a), b) and are only briefly summarized here.

A major problem for this model as applied to Archean and Paleoproterozoic terranes is the occurrence of a significant number of hypozonal (Gebre-Mariam et al., 1995) deposits worldwide that were deposited in mid- to upper-amphibolite facies domains, as demonstrated by Kolb et al. (2015) among others. For these deposits, the fluid source must have been >15 km (possibly up to 20 km) deep, not from devolatilization during upper-greenschist to amphibolite-facies metamorphism as proposed in the crustal metamorphic model. In addition, multiple sulfur isotopic compositions of Neoarchean orogenic gold deposits in Western Australia show that local supracrustal rocks did not supply significant sulfur for the deposition of gold-related sulfides in orogenic gold deposits. Rather, data from Selvaraja et al. (2017) and LaFlamme et al. (2018) imply that this sulfur was derived from a deep homogenized reservoir that contained recycled mass-independent fractionated sulfur (MIF-S) isotope signatures sourced from an Archean sub-crustal sediment reservoir.

Although Phanerozoic orogenic gold deposits comply with the crustal metamorphic model in that most significant mesozonal to epizonal deposits are recorded from turbidite-dominated greenschist-facies domains (Goldfarb et al., 2005) from which major ore elements could be more deeply derived (Pitcairn et al., 2006), there are exceptions. As summarized by Zhao et al. (2019) in a description of the Jurassic Danba hypozonal orogenic gold deposit from the north-western margin of the Yangtze Block, China, there are also late Carboniferous to early Permian orogenic gold deposits in the Massif Central of France (Bouchot et al., 2005) and in Upper Devonian turbidite-hosted orogenic gold deposits in Nova Scotia, Canada (Kontak et al., 1990; Ryan and Smith, 1998).

In addition, recent documentation of Chinese orogenic gold deposits, particularly those adjacent to the North China and Yangtze craton margins, has ruled out crustal metamorphism as a universally viable orogenic gold model. As summarized by Li and Santosh (2017) and Deng et al. (2020a), b), with a comprehensive list of previous publications, the most important orogenic gold event in the North China Craton was related to the Upper-Jurassic to Lower Cretaceous mantle lithosphere thinning and delamination due to the complex history and geometry of subduction related to convergence of the Paleo-Pacific Plate. This resulted in asthenosphere upwelling, widespread largely granite magmatism, and widespread mesozonal to epizonal orogenic gold mineralization (Goldfarb and Santosh, 2014; Yang and Santosh, 2020; Yang et al., 2016) at 120 Ma (Deng et al., 2020c; Zhang et al., 2020a) in the Jiaodong Gold Province which contains >35% (> 5000 t gold) of China's gold resource.

Deng et al. (2020b) provide evidence that the auriferous ore fluids were derived from metasomatized mantle lithosphere on the North China Craton margin that was fertilized during earlier Triassic subduction of gold-enriched pyritic sedimentary rocks from the northern margin of the Yangtze Craton. In the Cretaceous, subsequent asthenosphere upwelling related to complex subduction of the Paleo-Pacific plate is interpreted to have caused devolatilization of the metasomatized and fertilized mantle lithosphere to release auriferous ore fluids. These fluids advected via lithosphere-scale faults and were focused into subsidiary faults and shear zones to form the Jiaodong gold deposits. Fortunately, the deposits were preserved due to relatively slow exhumation despite the previous lithosphere delamination (Zhang et al., 2020a).

Other Chinese gold deposits on the margins of the North China and Yangtze cratons present similar, although more subtle, problems. For example, Goldfarb and Groves (2015) indicate significant timing problems for a crustal metamorphic model to form the mesozonal to epizonal orogenic gold deposits in the Triassic Qinling gold province (Chen et al., 2008). At the time of regional metamorphism, there were no previously un-metamorphosed voluminous source rocks that could have experienced fluid and metal liberation during amphibolite facies metamorphism, implicating an external deeply sourced fluid (Li et al., 2018). Similar arguments apply to the Huangjindong goldfield, hosted in Neoproterozoic slate, in the Jiangnan Orogen, Hunan (Zhang et al., 2020b) and to Upper Oligocene and Lower Miocene orogenic gold deposits in the NNW-trending Ailaoshan shear zone between the South China and Indochina Blocks in south-eastern Tibet, as summarized by Wang et al. (2020a) and references therein).

3. A coherent mineral system model for orogenic gold deposits

An orogenic-gold mineral system model that represents a coherent and universally applicable model (Wyman et al., 2016) is derived below in terms of the four key components: Fertility, Geodynamics, Architecture, and Preservation.

3.1. Fertility parameter

The Fertility parameter of the orogenic gold mineral system must be represented by a sub-crustal H_2O–CO_2 S-bearing fluid containing dissolved Au and associated metals such as Ag, As, Bi, Sb, Te and W. As discussed by Goldfarb and Groves (2015), there are few unequivocal indications of this precise fluid or metal source from multiple fluid inclusion, stable isotope, or radiogenic isotope studies because fluids have been modified by reactions along the long crustal pathways as they migrate towards gold depositional sites (Ridley and Diamond, 2000). The only obvious universal constraints are that the original fluid was almost certainly near-neutral and reduced (Goldfarb and Groves, 2015), although S isotope ratios of ore-related sulfides can, in some instances, discriminate between alternative sources (Wang et al., 2020b). Thus, the ultimate sub-crustal source of fluid and metals must be deduced from factors such as geodynamic setting and tectonic timing.

3.2. Geodynamic parameter

Orogenic gold deposits are invariably formed in accretionary or, less commonly, collisional tectonic environments related to subduction (Goldfarb et al., 2001; 2005), indicating that convergent margins are the critical dynamic setting. Such a setting can explain the late- to post-metamorphic timing in host sequences precisely when a change in far-field stresses promoted a change from compression to transpression or transtension, as demonstrated by

the geometry of the orogenic gold orebodies (Groves and Santosh, 2015; Groves et al., 2018). This implicates a fundamental relationship to a change in plate motion and stress regime on the whole-Earth scale induced by cessation of subduction, perhaps due to collision with a basement block or stalling of the slab during subduction (Seno and Kirby, 2014).

In a normal convergent margin setting, the only realistic sub-crustal source of fluid and metals is subducted oceanic crust and an overlying sediment wedge (Goldfarb and Groves, 2015; Goldfarb and Santosh, 2014; Groves and Santosh, 2016; Wyman et al., 2016). Devolatilization of a subducted slab can result in extensive upward fluid-flux along slab-mantle boundaries (Katayama et al., 2012; Peacock et al., 2011; Sibson, 2004) into fore-arc or accreting terrane margins. At this stage, the oceanic slab and pyrite-bearing sediment wedge will devolatilize releasing S together with Ag, As, Bi, Sb and Te to the fluid via breakdown of sedimentary pyrite to pyrrhotite (Large et al., 2009; Steadman et al., 2013). Such over-pressured fluids (Sibson, 2013) can then be transported as injection-driven seismic swarms (Cox, 2016) from the mantle lithosphere to crustal levels in lithosphere- to crustal-scale fault zones to eventually deposit orogenic gold deposits at even shallower levels in lower-order structures (Hyndman et al., 2015).

A schematic model, adapted from the Goldfarb and Santosh (2014) and Groves et al. (2020b) models is presented in Fig. 4a.

An adapted subduction-related model is required for orogenic gold provinces that are sited on craton margins as in eastern China. In their geodynamic model for the well-documented Jiaodong deposits, Goldfarb and Santosh (2014) suggested that the auriferous fluids could be derived indirectly from the mantle lithosphere wedge that had been fertilized and metasomatized by fluids derived from a subduction zone. Subsequent geochemical and isotopic syntheses by Deng et al. (2020a), b) have supported the latter model and shown that mantle-lithosphere metasomatism with possible anomalous enrichment in gold (Saunders et al., 2018) was related to an earlier subduction event. Similar models have been derived for the Ailaoshan gold province (Wang et al., 2020b), and previously postulated more generally by Bierlein and Pisarevsky (2008), Hronsky et al. (2012), and Wyman et al. (2016), among others. Groves et al. (2020a)) discuss the mechanisms that might allow advection of such deep fluids into the crust without partial melting to produce magmas. A schematic model based on Deng et al. (2020a), b) is shown in Fig. 4b and 4c.

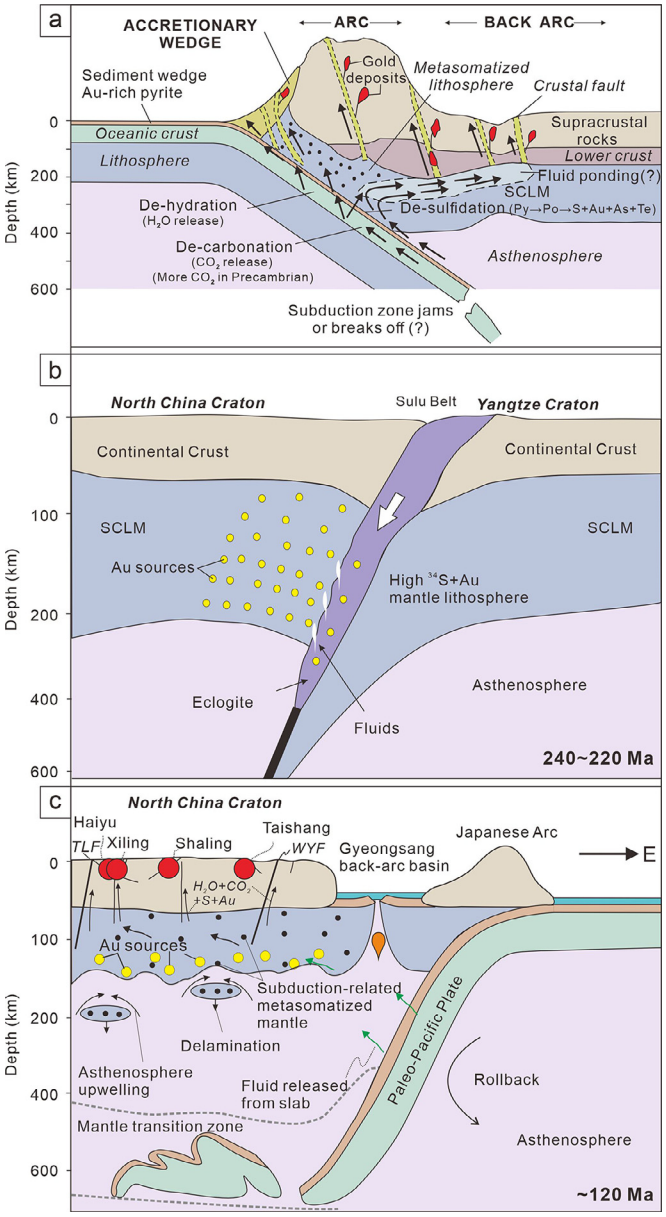

Fig. 4. Schematic representation of subduction-based models for ore-fluid source for orogenic gold deposits globally. A) direct subduction model adapted from Groves et al. (2020b). B) two-phase subduction model involving a metasomatized and fertilized mantle lithosphere source of fluid and metals adapted from Yang et al. (2021).

3.3. Architecture parameter: fluid plumbing system

For the mineral system orogenic-gold models in Fig. 4a and 4b, a lithosphere-crust continuum in structural architecture is required (McCuaig and Hronsky, 2014). The required lithosphere-scale structures are commonly marked by anomalous concentrations of lamprophyre dykes or felsic-intermediate intrusions with mantle source components (Witt et al., 2013) that indicate a lithosphere connection for fluid conduits (Perring et al., 1987; Rock et al., 1989). The first-order faults are most highly endowed where they are intersected by high-angle accommodation structures (Groves et al., 2018, 2020a, and earlier references within).

Common structural traps related to second-order subsidiary faults and shear zones include tight, thrusted antiforms, intersections between strike- extensive shear zones and high-angle fault corridors, commonly at jogs in the former, irregular sheared margins of small granite or other intrusions, and triple-point or quadruple-point junctions between adjacent intrusions (Fig. 5), as discussed by Groves et al. (2018). An excellent example of a control by quadruple-point granite intrusions is provided by the giant Hemlo orogenic gold system (Fig. 6) in an amphibolite-facies terrane where such controls are more common. Important chemical traps include fractured iron-rich host rocks and carbonaceous sedimentary units (Goldfarb and Groves, 2015). The hydrothermal systems also require caps to effectively impound fluid flux within the permeable trap zone. For Precambrian orogenic gold systems this is normally provided by relatively impermeable metasedimentary sequences that overlie more-permeable fractured volcanic sequences in greenstone belts (Groves et al., 2003), but there may be more subtle controls in Phanerozoic deposits.

3.4. Preservation parameter

For all mineral deposits, Preservation is as important as formation in dictating the distribution of deposits through time (Groves et al., 2005b). Orogenic gold deposits are anomalous in that they formed at crustal depths >2 km and

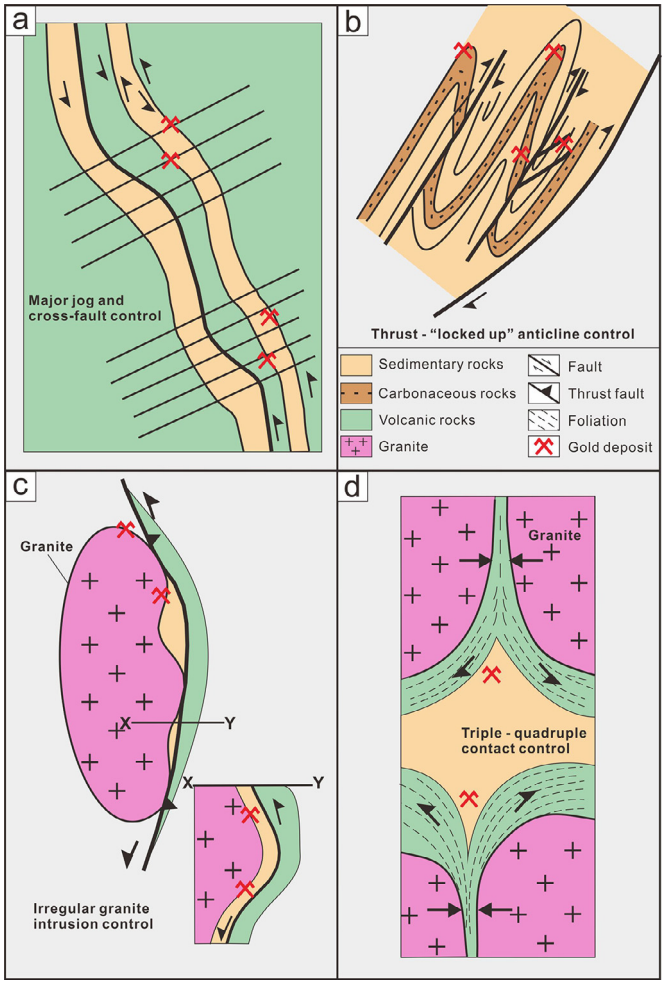

Fig. 5. Schematic diagrams showing repetitive structural architecture at fluid sinks or traps for orogenic gold systems: a) Major jogs on crustal-scale- and subsidiary faults/shear zones cut by corridors of accommodation faults; b) "Locked up" thrusted anticlinal folds; c) Irregular contacts on faulted margins of granite intrusions; d) Triple-and quadruple- point granite intrusion architecture. From Groves et al. (2020a)).

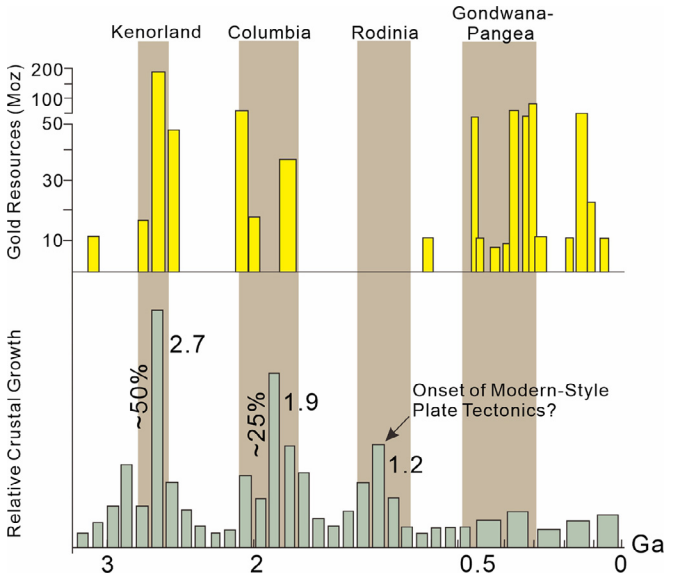

Fig. 7. Temporal distribution of orogenic gold deposits in terms of crustal evolution and development of supercontinents. Adapted from Goldfarb et al. (2001, 2005).

mostly >5 km (Goldfarb et al., 2005; Groves, 1993), and have improved preservation potential because of their late-orogenic timing after the major compressional phase of tectonism (Goldfarb et al., 2001: their Figs. 3, 4). Both Precambrian deposits and Phanerozoic deposits on craton margins were preserved because of thick buoyant sub-continental lithosphere keels beneath them (Griffin et al., 2013, 1998; Groves et al., 2005b; Wyman and Kerrich, 2002) or adjacent to them (Zhang et al., 2020a). Orogenic gold deposits thus formed during most orogenic events in Earth history (Fig. 7). The global distribution of exhumed high-grade metamorphic roots to Mesoproterozoic to early Neoproterozoic orogenic belts explains the absence of orogenic gold deposits (Fig. 7) during this billion years of Earth history (Goldfarb et al., 2001).

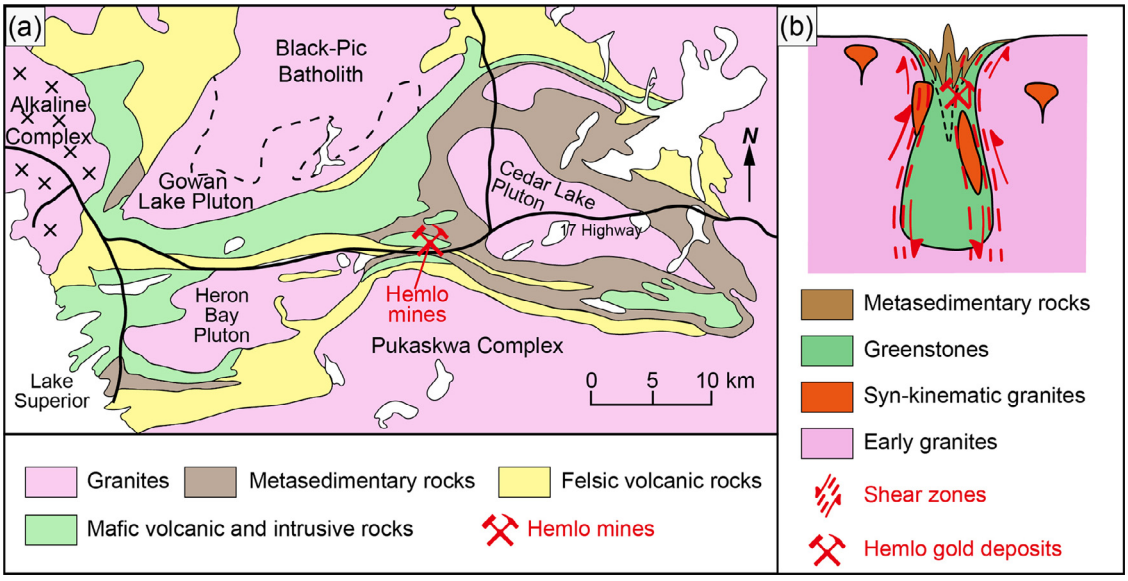

Fig. 6. Control of orogenic gold deposits by structural and resultant strain complexities due to quadruple granite intrusion geometry in amphibolite-facies terranes. Example is provided by the giant Hemlo group of deposits in the Superior Province, Ontario, Canada. Schematic cross section resembles an upward flower structure. Adapted from Muir (1997) and Lin and Beakhouse (2013).

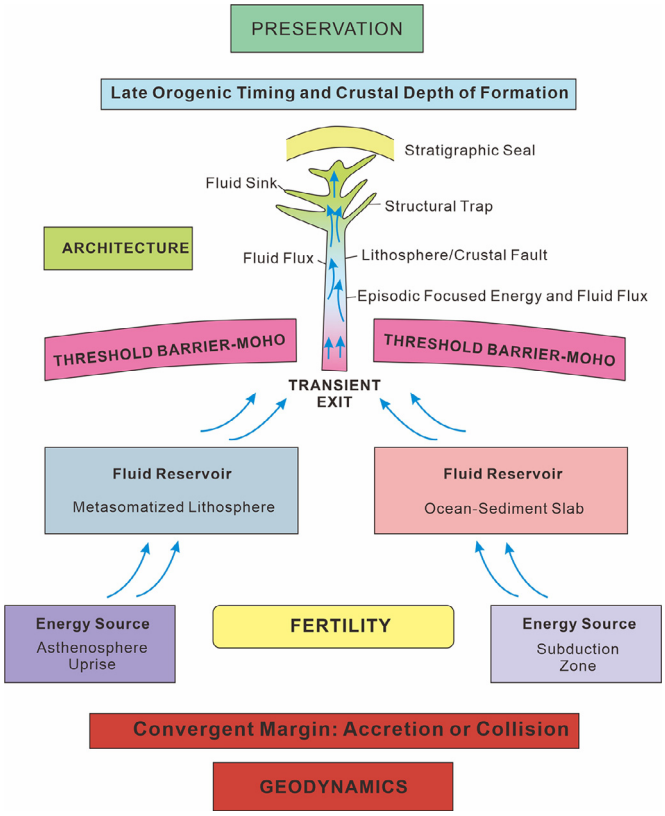

Fig. 8. Schematic self-organising critical orogenic gold mineral system showing alternate fertility sources that have the same basic architecture parameters. Adapted from Groves et al. (2020a)) based on Wyman et al. (2016).

3.5. Summary

A schematic summary of the orogenic gold mineral system is shown in Fig. 8 with two alternative models for the Fertility parameter.

4. Critical mineral-system-based exploration criteria for orogenic gold deposits

The critical components of the mineral-system orogenic-gold model (Fig. 1) relevant to exploration are exhaustively discussed in logical order from Geodynamics to Fertility to Architecture to Preservation and summarized in a series of Tables that include geophysical and geochemical proxies by Groves et al. (2020a)). Consequently, only those most important exploration criteria that specifically depend on a sub-crustal rather than crustal mineral system model are briefly outlined below.

As discussed above, the critical Fertility and Geodynamic factors are related to the subduction of an oceanic slab and overlying sediment wedge that can provide fluid, sulfur, gold, and other ore metals to the orogenic gold system (Figs. 3 and 4). As subduction is effectively linked to convergent margin geodynamic settings, these must be identified as crucial terranes or provinces within which to target gold exploration. One of the useful geological tools to distinguish extinct convergent margins from surface geology is the recognition of Ocean Plate Stratigraphy (OPS), even in Precambrian terranes (Kawai et al., 2009). The OPS has been defined as the original composite stratigraphic succession of the ocean floor which is incorporated in an accretionary complex and can be considered as the travelogue of an oceanic plate from mid oceanic ridge to subduction zone (Safonova et al., 2009; Santosh, 2010). A typical OPS

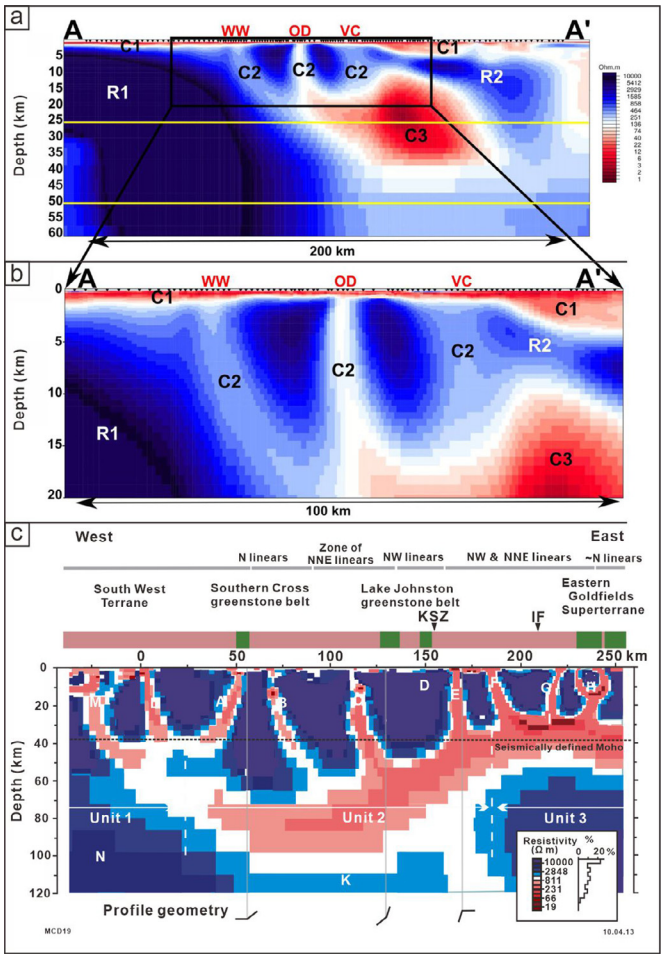

Fig. 9. A) Magnetotelluric survey from the Gawler Craton IOCG province from Heinson et al. (2018). a) Resistivity to 60 km depth. b) enlargement of central area to 20 km depth. High conductivity structure C3 (possible high fluid-flux alteration zone) is sited on Gawler Craton margin at 15–40 km depth (down to top of MOHO). Low resistivity pathways C2 extend from C3 to the surface, pointing to known IOCG deposits. The strongest central pathway points to the giant Olympic Dam deposit. These anomalies have been termed "The Fingers of God". B) Magnetotelluric section across the greenstone belts and crustal-scale faults of the Yilgarn Block. From Geological Survey of Western Australia, 2011. Image courtesy of the Geological Survey and Resource Strategy, Department of Mines, Industry and Safety @ State of Western Australia. Image modified in terms of color codes to match A).

sequence, accreted on to land, would thus be a sequence of MORB, chert, OIB, and trench sediment (Isozaki et al., 2010), with more complex variants in Phanerozoic collisional belts and Precambrian greenstone belts, as summarized by Groves et al. (2020a)).

At the province or terrane scale, the Architecture parameter of the mineral system model is linked to the Geodynamic and Fertility factors. The key Architecture factor at this scale is provision of major permeable structures that extend to the MOHO and can deliver high thermal and seismically driven fluid flux from lithosphere to the crust (Figs 3 and 4). For well-endowed gold provinces these are the steeply dipping first-order faults and shear zones that are marked by distinct aeromagnetic lineaments and commonly control the distribution of lamprophyres and related intrusions. Magneto-telluric sections (Dentith et al., 2013) most clearly mark the vertical extent of these lineaments. Recent studies by Heinson et al. (2018) on the Gawler Craton, South Australia (Fig. 9a and b) define a high conductivity structure C3, a possible high fluid-flux alteration zone, on the craton margin at 15–40 km depth, down to the top of the MOHO. Low resistivity pathways C2 ex-

tend from C3 to the surface, pointing to known IOCG deposits with the strongest central pathway below the giant Olympic Dam deposit. These anomalies have been termed "The Fingers of God" (Robertson and Thiel, 2019). Although these "Fingers of God" are defined for IOGD deposits, reconnaissance magneto-telluric surveys over the greenstone belts of the Yilgarn Block, Western Australia (Fig. 9c) show similar channel ways extending to the MOHO with lowest resistivity zones below the Eastern Goldfields, and poorly defined "Fingers of God" below the most eastern, most highly gold-endowed terrane in the Yilgarn Block. Thus magneto-telluric surveys have the potential to directly detect zones of high fluid flux and fluid-rock reaction for hydrothermal deposits with sub-crustal fluid sources, such as orogenic gold mineral systems.

Terranes with low-strain low-permeability sequences with such widely spaced high-strain high-permeability lithosphere-scale shear zones provide greater opportunity for the formation of world-class to giant mineral systems, because high fluid flux is focused into a relatively small volume within the terrane (Groves et al., 2000). More rapid uplift contemporaneous with gold mineralization, as indicated where late conglomerate basins are juxtaposed against lower volcanic sequences (Abitibi Belt, Canada: Colvine et al., 1984; Norseman-Wiluna Belt, Western Australia: Tripp, 2014), may also be an important regional factor. These are interpreted to signify sites of anomalously rapid uplift rates along the first-order structures, where lowering of lithostatic pressures in interconnecting faults enhances hydro-fracturing, extreme pressure fluctuations, and effective gold deposition through fluid phase separation episodes (Groves et al., 1987).

Importantly, the sub-crustal mineral system allows amphibolite-facies domains to be valid exploration targets for hypozonal orogenic gold deposits, thus expanding viable exploration space. Although not exclusive to hypozonal deposits, they are commonly located in more complex structural geometries that are developed at triple- to quadruple-point junctions between three or more granite bodies that impinge on the volcano-sedimentary sequences that they have intruded. Hypozonal (for example, numerous examples from the Southern Cross belt of Western Australia; Eleonore, Musselwhite, and Hemlo in Canada, and less common mesozonal (for example Red Lake in Canada; deposits in the Quadrilatero of Brazil) gold deposits are located along strain gradients in heterogeneous stress zones within inverted V-shaped or cuspate volcano-sedimentary segments of belts.

From an exploration viewpoint, these triple- and even quadruple-point junctions are evident on available aeromagnetic images and are commonly located on gravity gradients, as for many other orogenic gold deposits (Bierlein et al., 2006b) due to magnetic susceptibility and density contrasts between granite intrusions and supracrustal sequences, particularly in Precambrian greenstone belts.

District- to deposit-scale repetitive structural geometries and fluid caps that control the location of many orogenic gold deposits are described and discussed in considerable detail by Groves et al. (2018) and Hronsky (2020) and are only summarized here (Fig. 5). In terms of their Preservation factor, orogenic gold systems are anomalous in that they can form at deep crustal levels and may individually, like the giant Kolar hypozonal deposit (Radhakrishna and Curtis, 1999; Sarma et al., 2011), extend to > 2 km down dip or plunge, explaining their distribution throughout most of geologic time (Goldfarb et al., 2001). Whether epizonal, mesozonal, or hypozonal groups of deposits (Gebre-Mariam et al., 1995) are dominant in a terrane provides a geological estimate of the degree of exhumation and hence its exploration potential. A terrane having mostly epizonal Au-Sb deposits, for example, clearly has the potential to host deeper mesozonal deposits.

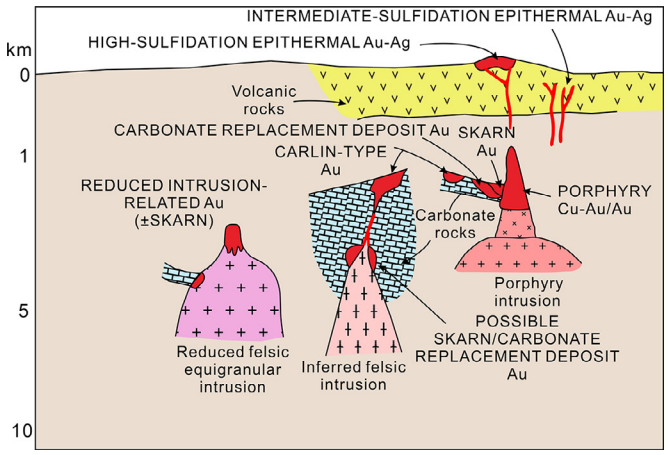

Fig. 10. Schematic representation of porphyry-related system including skarns. Other skarns related to Carlin-Type gold deposits and Reduced Intrusion-Related gold deposits or IRGDs are excluded from the discussion of porphyry-related systems. Modified from Sillitoe (2010).

5. Genetic model for porphyry-related deposits

5.1. Introduction

Although porphyry Cu-Au-Mo (Seedorff et al., 2005), high-sulfidation Au-Ag (Sillitoe and Hedenquist, 2003), and skarn Fe-Cu-Au-Mo-Sn-W (Meinert et al., 2005) deposits are commonly reviewed as distinctive deposit classes, it is potentially their combination in porphyry-related deposits which aids district-scale mineral exploration (Sillitoe, 2010). As shown in Fig. 10, porphyry and high-sulfidation epithermal deposits commonly form a continuum, whereas skarns may also be associated with other hydrothermal systems such as IRGD and Carlin-type deposits wherever there are reactive, normally carbonate, rocks in the host sequences. Only those skarns spatially related to porphyry-related systems are considered here.

5.2. Coherent genetic model

Unlike orogenic gold deposits where development of a coherent mineral system has been difficult because of lack of consensus, particularly agreement about fertility factors, porphyry-related deposits have been widely accepted as derived from magmatic-hydrothermal fluids from porphyry bodies that lie adjacent to, or below, the ore deposits in volcanic, island, and continental arcs in convergent margins (Sillitoe, 2010, 2020). The deposits are normally associated with small-volume finger-shaped and composite plugs or, more rarely, dykes, ranging from porphyritic diorite to granite in composition, that represent late stages of multiple magma pulses released from fractionating upper crustal magma chambers. Porphyry Cu-Au±Mo deposits are typically emplaced at paleo-depths of about 1–6 km (Seedorff et al., 2008) above large composite plutonic complexes that formed during major intrusive events. High salinity, low pH, high temperature, and overpressured magmatic-hydrothermal fluids are exsolved from these intrusions following their crystallization. These fluids initiate hydraulic fracturing both of their carapace and country rocks, leading to fluid phase separation, complex wallrock reactions, and hydrothermal alteration zoning (Heinrich, 2005). Multiple magmatic-hydrothermal pulses produce different overprinting stages of quartz-sulfide bearing stockwork veins, hence increasing their metal grades. During progressive cooling of the waning hy-

drothermal system, the composition of late-stage fluids shifts towards higher pH conditions. These late-stage fluids typically overprint the early-stage alteration zones, especially along deposit-scale structures (Heinrich, 2005 and references therein).

As discussed in more detail below, the initial key development in the formulation of a mineral system model that had exploration relevance was the evolution from viewing individual porphyry Cu-Au-Mo deposits as discrete isolated bodies to the integration of their distinct geochemical and alteration zonation to developing a coherent zoned-alteration model as documented by Lowell and Guilbert (1970). This was followed by the incorporation of many porphyry Cu-Au-Mo deposits with high-sulfidation Au-Ag deposits, and some Fe-Cu-Au-Ag skarns, into a combined porphyry-related geological and alteration model, as summarized by Sillitoe (2010, and references therein). More sophisticated modelling of the geometry of subduction zones and their related structural architecture (Hayes et al., 2018) led to a better understanding of the spatial occurrence of porphyry-related systems, and geochemical fingerprinting of fertile intrusions aided the discrimination between highly prospective and less prospective intrusive belts (Loucks, 2014). Hence, although mineral system models are not specifically referenced, it is possible to develop a single integrated mineral system model for three related mineral deposit classes using the seminal review of Sillitoe (2010) as a basis.

6. A coherent mineral system model for porphyry-related deposits

As for the orogenic gold deposits, the mineral system for porphyry-related deposits is developed in terms of the four critical parameters: Fertility, Geodynamics, Architecture, and Preservation. In this case, Geodynamic settings are described first, to provide context to Fertility factors.

6.1. Geodynamic parameter

Porphyry-related systems are exclusively related to subduction-related convergent margin settings, particularly where there is an extended and/or complex subduction history (Clark et al., 1982; Jankovic, 1977; Lowell, 1974; Sillitoe, 1972; Waite et al., 1997). The porphyry Cu-Au-Mo and associated high-sulfidation epithermal Au-Ag and skarn Cu-Au-Fe system is the most prominent mineral system formed during the early evolution of convergent margins (Hedenquist et al., 2012).

At the global scale, individual clusters of porphyry-related systems are normally sited along specific strike-extensive curvilinear segments of arcs at spacings of 10 s to 100 s of kilometres (Fig. 11:Sillitoe and Perello, 2005), especially where they are intersected by cross-cutting regional structures (Gow and Walshe, 2005; Salfity, 1985). In an important link to Architecture, locations of these inter-related deposits (Sillitoe, 2010, 2020) are normally the result of conjunction of flat subduction slab compression (Espurt et al., 2008) and oblique, deep extensional transform or accommodation faults (Fox et al., 2015; Wilkinson, 2013), with systems structurally controlled by intersecting crustal- to lithosphere-scale fault structures (e.g., Chuquicamata-Radomiro Tomic and Escondida clusters, Chile: Gow and Walshe, 2005; Matteini et al., 2002) or pull-apart basins (e.g., Peschanka cluster, Russia: Chitalin et al., 2021). Fig. 12, adapted from Sun et al. (2015) shows a type example of controlling structural components.

Although emphasis is placed on the continental arcs of the Andes in terms of Figs. 11 and 12, other porphyry-related systems in southeast Asia and the southwest Pacific are dominated by island arcs that contain over 160 early- to middle-Miocene and Pliocene-Pleistocene porphyry-related Cu-Au systems. These have many similarities in terms of Geodynamics, Fertility, Architecture, and Preservation to equivalents in the Andes (Fig. 13). As summarized by Garwin et al. (2005), they are typically situated in zones of complex subduction geometry that result from multiple events involving polarity reversals, arc-arc and island arc-continent collisions, rifting, and transcurrent faulting. As in the Andes (Figs. 11 and 12), porphyry-related Cu-Au districts are related to bends and tears in down-going subduction slabs (Müller et al., 2002) with ore districts located near high-angle arc-transverse faults across the arcs (Fig. 13:Corbett and Leach, 1998; Gow and Walshe, 2005).

Deposits within the porphyry-related system normally have a close spatial and genetic relationship to high-level (<5 km depth) complexes of oxidized and porphyritic calc-alkaline granites (*sensu lato* throughout), some of which are highly potassic or even alkaline (Müller and Groves, 2019 and references therein) in volcanic and continental arcs. The fertile intrusions were largely emplaced during periods of mild compression with limited volcanism, which may pre-date or post-date the intrusive activity (Mpodozis and Cornejo, 2012). There is also an important group of porphyry systems related to continent-continent collision in the Tethyan belt from Iran to Tibet (Deng et al., 2021; Wang et al., 2020c), which is further discussed in the section on craton margins below in terms of magmatic-hydrothermal systems associated with metasomatized mantle lithosphere.

6.2. Fertility parameters

Calc-alkaline porphyry-related systems have no specific igneous rock association, with fertile intrusions ranging from diorites though granodiorites to granites. Porphyry Cu deposits hosted by high-K calc-alkaline or shoshonitic intrusions can range from monzodiorites through monzonites to quartz-monzonites and monzogranites, (Müller and Groves, 2019 and references therein).

Compositions of gold-fertile arc-basalt magmas (Loucks, 2014) define the source of the porphyry systems as gold-enriched metasomatized mantle lithosphere fertilized via low-degree partial melting of deeper mantle during earlier, possibly subduction-related, thermal events (Tatsumi and Eggins, 1995), implicating a dual subduction association in contrast to other arc settings (Waters et al., 2021). The higher gold contents of more alkaline porphyry systems (Müller and Groves, 2019) support such a model, as do zircon compositions from fertile porphyry systems (Bao et al., 2018) that implicate anomalously water-rich source magmas (Lu et al., 2016), that degas sulfur (Dilles et al., 2015).

In subduction-related arc settings, it appears that devolatilization and partial melting of the subducted oceanic slab metasomatically enriches the mantle wedge in LILE and volatiles such as H_2O and Cl (Bekaert et al., 2021). Adiabatic decompression melting of these enriched mantle lithosphere domains produces uprising basic H_2O- and LILE-enriched magmas with high oxidation states, typically >1 log degree above the FMQ buffer (Lee et al., 2005; Müller et al., 2001, 2002; Li and Audetat, 2013). Recent studies by Williams et al. (2018) imply that high oxidation states of a magma are generally correlated with high magmatic H_2O contents. These uprising melts can form significant magma chambers in the crust where ongoing crystal fractionation and the continued replenishment by additional injections of basic mantle melt leads to the release of evolved magmatic pulses from the top part of the chamber (Halter et al., 2002; Hattori and Keith, 2001; O'Hara and Mathews, 1981; Ulrich et al., 2001). These pulses of fertile magma, with high whole-rock Sr/Y, V/*Sc*, La/Yb, Fe_2O_3/FeO and Eu/Eu* ratios, are capable of forming the porphyry Cu-Au-Mo and related high-sulfidation epithermal- and skarn systems, typically at depths between 3 and 5 km beneath the paleo-surface (Müller and Groves, 2019 and references therein). Their economic significance

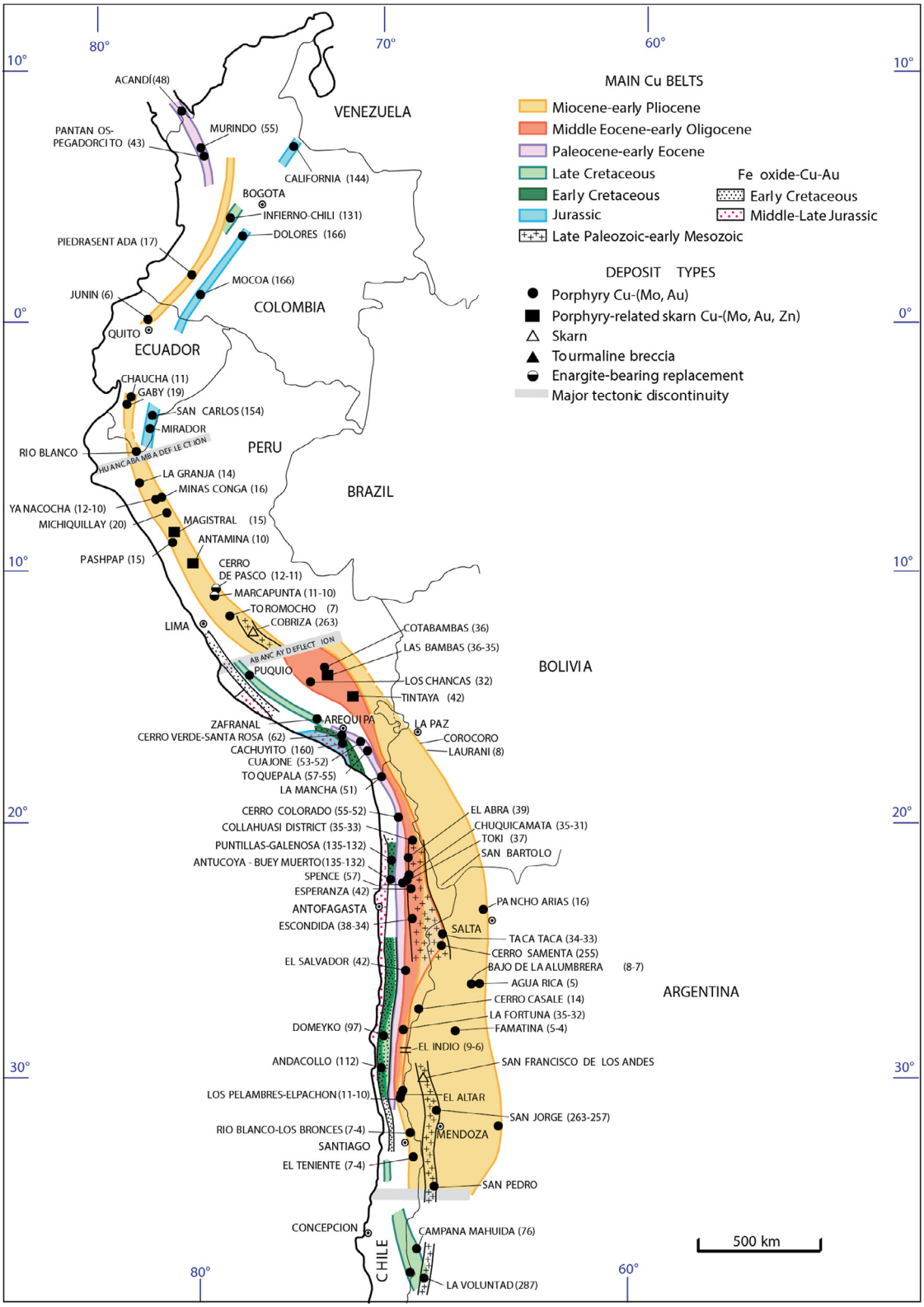

Fig. 11. Geodynamic setting of porphyry-related Cu-Au-Mo systems along the strike-extensive curvilinear continental arcs of the Andes. Porphyry-related systems formed from Jurassic to early Pliocene as shown by coloured main copper belts. Modified from Sillitoe and Perello (2005).

depends on their metal associations and grades as well as their exposure levels relative to the current land surface. Gold-rich porphyry Cu deposits are normally hosted by intermediate intrusions (diorites or monzodiorites, depending on the magma series), whereas porphyry Mo deposits are associated with more evolved intrusive phases, such as granites or monzogranites, commonly involving significant crustal contamination (Sillitoe, 1979, 2000; Audetat and Li, 2017; Huang et al., 2018; Zhang et al., 2021). Microthermometric studies also suggest shallower average formation depths for porphyry Cu-Au deposits (2.1 km; Sillitoe, 2000) compared to the average depth of porphyry Cu-Mo deposits (3.7 km; Murakami et al., 2009).

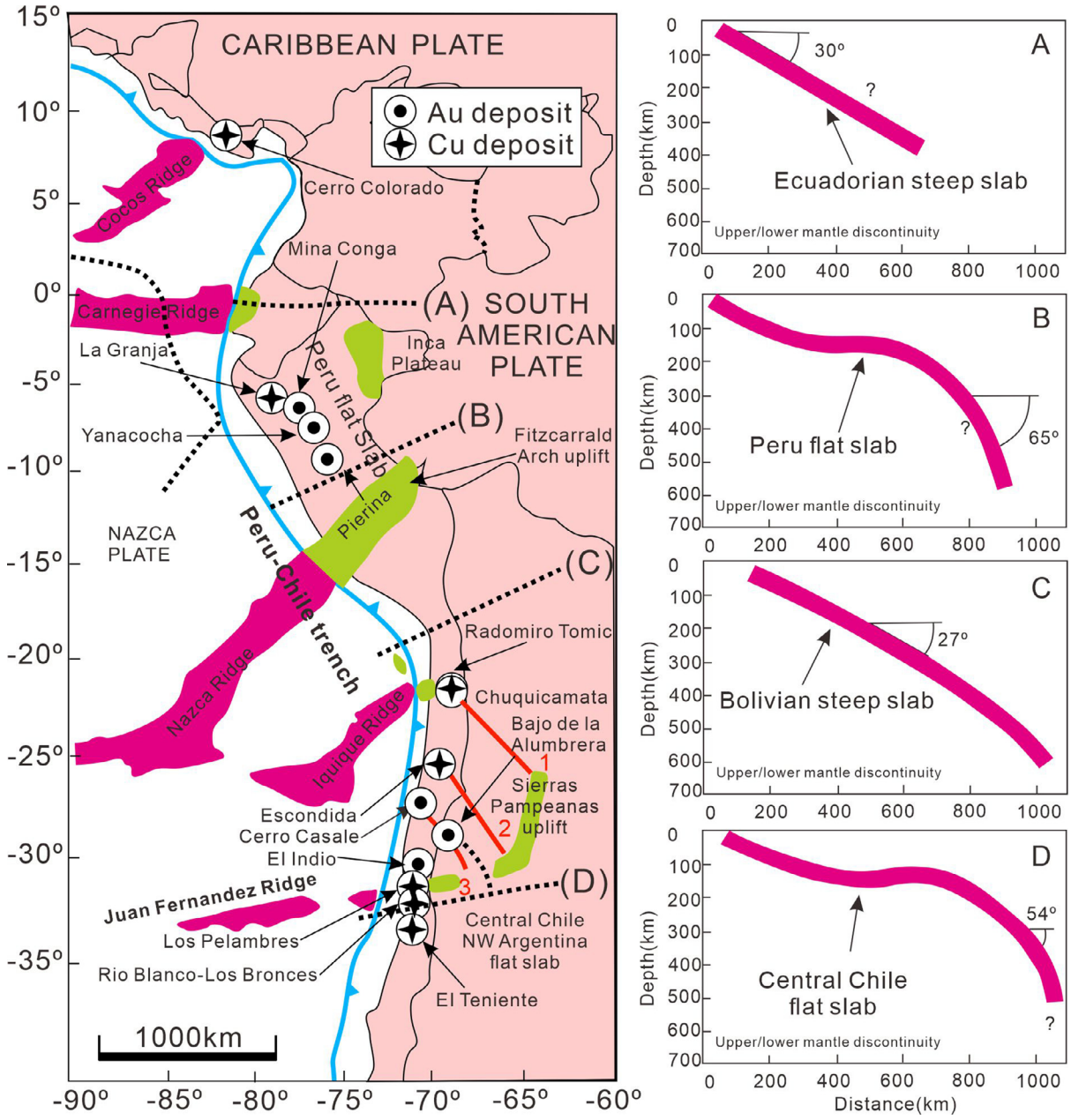

Fig. 12. Province-district scale Architecture showing location of porphyry-related systems in shallow slab domains at intersection between arc-parallel faults and oblique faults. Adapted from Salfity (1985) and Sun et al. (2015) who suggest that large porphyry Cu clusters are closely associated with ridge subduction and/or intersections of deep-seated structures. Subduction of young ridges is the most favourable geologic process for slab melting in the Cenozoic, forming highly oxidized melt with high initial Cu contents. Red lines represent NW-trending lineaments from Salfity (1985): 1. Calama-El Toro; 2. Archibarca; 3. Culampaja.

6.3. Architecture

The district to deposit scale Architecture of porphyry-related systems is shown schematically in Fig. 14. Normally, a cluster of porphyry intrusions, including the mineralizing porphyry, cut the underlying non-porphyritic host batholith, and extend into the overlying volcano-sedimentary arc sequences. There may be peripheral diatreme-maar complexes and intrusion breccias caused by volatile degassing of the magmatic system (Fig. 14a). The vertically and laterally zoned alteration comprises early sodic-calcic alteration typically at the root zones of porphyry systems, cut by central potassic alteration zones with widespread flanking propylitic alteration assemblages, whose full extent may only be realized through trace element contents of epidote and chlorite intersected in exploration drillholes (Wilkinson et al., 2020). Sericitic, chloritic, and argillic alteration zones lie above and flanking the core potassic zone, with all overlain by a lithocap within the overlying andesitic to dacitic volcanic and tuffaceous carapace (Fig. 14b). In places, especially along structures, sericite alteration can overprint early-stage potassic alteration assemblages during the waning stages of the cooling hydrothermal system. Higher temperature porphyry Cu-Au-Mo deposits are centred on the potassic alteration zone with overlying lower temperature high-sulfidation Cu-Au-Ag deposits and flanking intermediate-sulfidation Au-Ag deposits. Iron-rich host rocks appear most favourable for high-grade Cu-Au ores due to reduction of fluids along lithological contacts (e.g., Oyu Tolgoi, Mongolia: Crane and Kavalieris, 2012), with proximal Cu-Au and distal Au-Zn-Pb skarns developed in carbonate horizons (e.g., Ertsberg, Papua New Guinea: Prendergast et al., 2005). There may also be distal Zn-Pb-Ag carbonate replacement or vein deposits, with rare associations that include As, Au, Hg, Sb and W (e.g., Beiya, Yunnan province, China: Fu et al., 2017). This

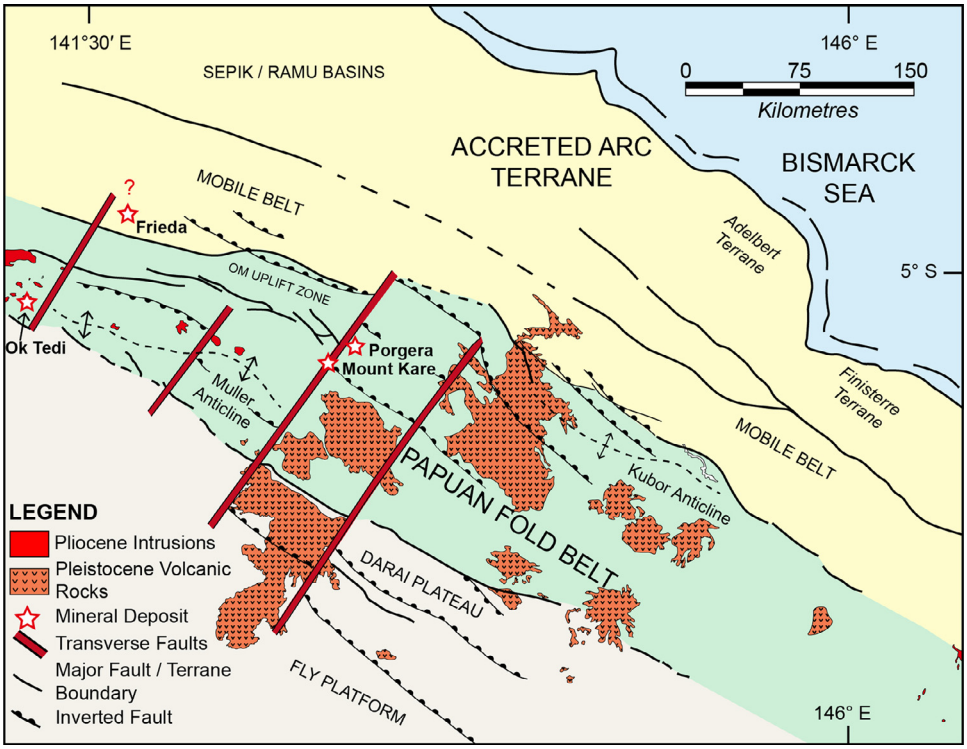

Fig. 13. Summary of the main tectonic and structural elements of the Papuan Fold Belt and associated world-class to giant epithermal Au and porphyry Cu-Au systems within the arc-continent collision zone of the Papua-New Guinea segment of the arc systems of the southwest Pacific margin. Deposit locations controlled by high-angle arc-transverse structures identified from offsets in basement-penetrating faults. Adapted from Gow and Walshe (2005).

produces a district-scale lateral zonation from Cu-Au-Mo to Au-Ag-Zn-Pb on the kilometre scale, with the porphyry-related system occupying many cubic kilometres of the crust (Halley, 2020).

Porphyry Cu-Au-Mo systems may be regarded as natural vertical pumps of hot magmatic-hydrothermal fluids within the upper crust. The classic zoned combined alteration and mineralization (Halley, 2020) represents the cooling of magmatic-hydrothermal fluids from $<700^0$C to $<250^0$C, with evolution from high-T two-phase highly saline fluids responsible for potassic alteration, proximal skarns, and Cu-Au+/- Mo ores to the development of overlying and lateral alteration zones with Au-Ag-Zn-Pb ores formed from lower-T single-phase, lower salinity fluids (Heinrich, 2005). Cooling of the giant hydrothermal system, combined with uplift and paleosurface degradation, leads to telescoping of the system by complex overprinting of early alteration and high-T ores by lower-T alteration and ores (Sillitoe, 1994). Thermochronology research discussed by McInnes et al. (2005) suggests that the hydrothermal systems evolved within periods of <100,000 years, as also suggested by Mercer et al. (2015).

6.4. Preservation

Unlike orogenic gold systems that generally formed at >5 m depth during the waning phase of compression and tectonic shortening in the host convergent margin, porphyry-related systems normally formed at shallower depths and much earlier during an early transient extensional-compressional phase which would be followed by extreme tectonic shortening and uplift (Mpodozis and Cornejo, 2012). Thus, preservation is a critical factor. Holocene uplift rates in arcs calculated from geomorphological features can range up to 1 to 5 km per million years (Remirez-Harraera et al., 2021). Calculations for several world-class porphyry Cu-Au systems using thermochronology by McInnes et al. (2005) suggest uplift rates of 0.26 to 0.72 km per million years. It is thus not surprising that porphyry-related systems only rarely extend back beyond the Miocene (Fig. 15) with older Upper Jurassic to Cretaceous examples largely represented by post-collisional arcs (e.g., Pebble, Alaska: Olson et al., 2017) and intra-continental Cu-Au or Mo±W porphyry-systems sited close to the North China and Yangtze craton margins in eastern China and Tibet (Mao et al., 2013).

There are rare older porphyry-related systems with subeconomic examples recorded from the Paleoarchean to Mesoarchean greenstones belts in the Pilbara Craton, Western Australia (Barley, 1982). The giant Neoarchean Boddington Cu-Au-Mo-Ag deposit in a low metamorphic grade greenstone belt lying on high-grade gneisses in the southwest Yilgarn Craton, although considered enigmatic (Turner et al., 2020), has many features of diorite-associated porphyry systems, including the metal association, high-T alteration assemblages derived from high-T high-salinity ore fluids, and strong lateral zonation. It is most likely hosted by a Neoarchean arc thrust back on to Paleoarchean metamorphic basement with thick mantle lithosphere, explaining its anomalous preservation.

A schematic summary porphyry-related mineral system model is presented in Fig. 16.

7. Critical mineral system-based exploration criteria for porphyry-related systems

Exploration criteria for porphyry-related mineral systems can be broadly considered using a hierarchical approach from global through province to district and deposit scales. At the global scale, due to Preservation issues, Cenozoic volcanic and continental arcs in convergent settings are preferred Geodynamic settings, although Mesozoic post-collisional arcs adjacent to stable craton margins are alternative settings. There may be rare older Geodynamic settings where segments of ancient arcs are tectonically preserved on older cratonic blocks.

Arcs that are metallogenically fertile for porphyry-related systems can be distinguished from less-prospective arcs by geo-

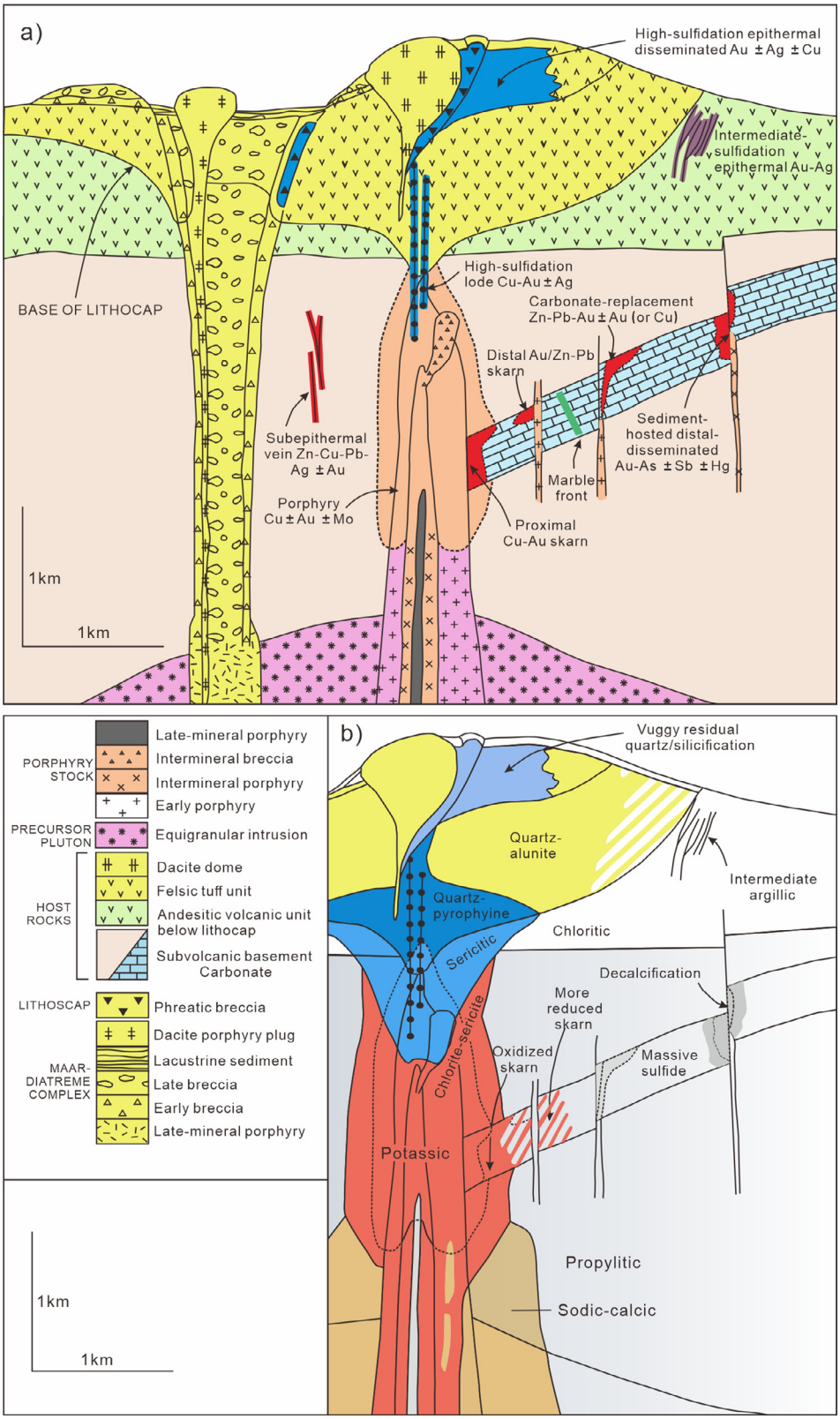

Fig. 14. District-deposit scale Architecture of a porphyry-related system. A) Anatomy of a telescoped porphyry-related system showing spatial interrelationships of a centrally located porphyry Cu ± Au ± Mo deposit in a multiphase composite porphyry stock and its immediate host rocks; peripheral proximal and distal skarn, carbonate-replacement, and sediment-hosted deposits in a carbonate unit and sub-epithermal veins in noncarbonate rocks; and overlying high- and intermediate-sulfidation epithermal deposits in and adjacent to the lithocap environment. The legend reflects the temporal sequence of rock types. B) Generalized alteration-mineralization zoning pattern for telescoped porphyry-related systems, based on the geologic and deposit-type cartoon in A). Note that shallow alteration-mineralization types consistently overprint deeper ones. Volumes of the different alteration types vary markedly from deposit to deposit and sericitic alteration and chlorite-sericite alteration tend to be more abundant in porphyry Cu-Mo deposits and porphyry Cu-Au deposits, respectively. Where there are strong structural components, alteration-mineralization in the lithocap is more complex than shown. Adapted from Sillitoe (2010).

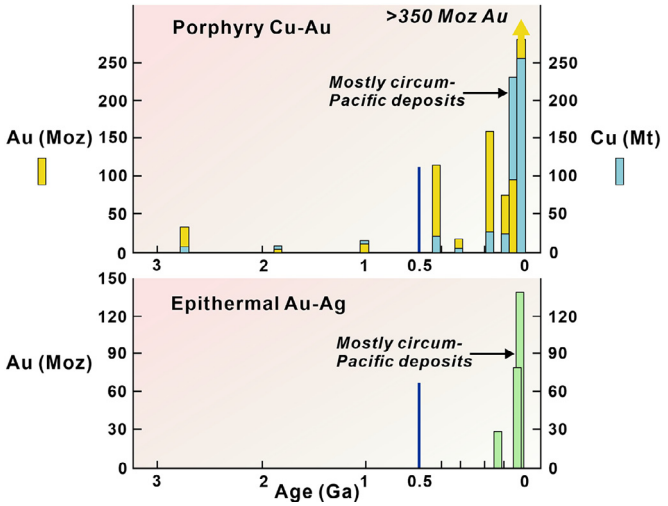

Fig. 15. Distribution of porphyry-related Cu-Au systems and epithermal systems with time. Adapted from Groves et al. (2005a, b).

chemical parameters of their volcanic components such as high Sr and V and anomalously low *Sc* and Y contents that relate to long-lived residence of periodically replenished mantle-derived magmas near the mantle lithosphere-crust boundary (Cocker et al., 2016; Loucks, 2014). A recent study on the use of whole-rock La/Yb ratios in the subduction-arc settings in British Columbia, Canada, and the Sierra Nevada, California, by Profeta et al. (2015) reveals their potential use as proxies for crustal thickness. Importantly, Profeta et al. (2015) confirm previous studies from northern Chile suggesting that increasing La/Yb ratios in arc rocks in the Chilean Andes, ranging from late Cretaceous to late Eocene, reflect a gradually thickening arc crust (Haschke et al., 2002; Kay et al., 1994). An improved understanding of the crustal thickness has important implications for global mineral exploration, because empirical studies reveal that economic porphyry copper deposits in the Chilean Andes and in the eastern Tethyan orogen are preferentially hosted by intrusions formed by partial melting of relatively deep mantle sources beneath a thickened lower crust where garnet remains as a stable residual phase in the mantle (Cocker et al., 2016; Haschke et al., 2002; Hollings et al., 2005; Jamali, 2017; Loucks, 2014). Importantly, the parental intrusions of the Oligocene Chuquicamata intrusive complex, which hosts the giant Chuquicamata and Radomiro Tomic porphyry copper deposits in northern Chile, are characterized by distinctly high whole-rock La/Yb ratios of >19 reflecting a crustal thickness of about >30 km (Cabrera, 2011). By contrast, poorly mineralized Triassic arc intrusions in northern Chile are defined by low La/Yb ratios of <19 that are interpreted to reflect partial mantle melting beneath a relatively thin crust during the initial period of subduction in the Chilean continental arc.

It is well accepted that the granite stocks or cupolas associated with porphyry Cu-Au deposits are generally oxidized and magnetite-bearing (Cao et al., 2018; Ishihara and Chappell, 2010). Oxygen fugacity or the oxidation state of magmas is a fundamental thermodynamic property that both governs the redox equilibria in solid Earth systems (Williams et al., 2018) and determines the speciation of volatiles in the upper mantle (Aulbach et al., 2017). Recent studies reveal that melts and hydrothermal fluids with elevated oxidation states are favourable for Cu solubility (Lee et al., 2012; Li et al., 2017). The oxidation state of intrusions can be estimated from whole-rock Fe_2O_3/FeO ratios (Blevin, 2002). Studies on Paleozoic granites from the Lachlan Fold Belt in Australia reveal that intrusions that are spatially associated with porphyry Cu-Au mineralization at the Cadia and Northparkes mines have whole-rock Fe_2O_3/FeO ratios of >1 (Blevin, 2002). However, as this method is restricted to fresh, unaltered, and unweathered intrusions, the use of whole-rock Eu/Eu* ratios represents an alternative method to estimate the oxidation state of igneous intrusions (Dilles et al., 2015; Lee et al., 2017; Loader et al., 2017) as a rise in the oxidation state of the magma converts Eu^{2+} to Eu^{3+} (Hao et al., 2017). Oxidized intrusions that are associated with porphyry Cu-Au deposits typically have elevated whole-rock Eu/Eu* ratios of ≥1 (Lee et al., 2017). Lee et al. (2005) and Olson et al. (2017) also define a positive correlation between the oxidation state of the magma and whole-rock V/*Sc* ratios. Hence, elevated oxygen fugac-

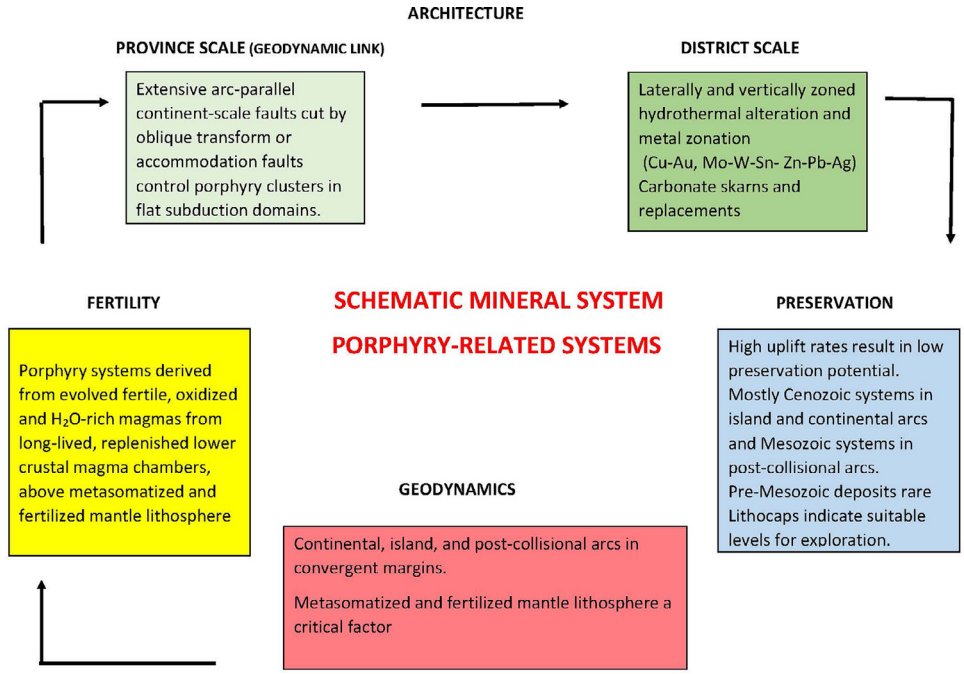

Fig. 16. Schematic mineral system model for porphyry-related systems in terms of Geodynamics, Fertility, Province-scale Architecture, District-Deposit-scale Architecture, and Preservation.

ities of arc lavas exceeding +1.0 log unit above the FMQ buffer are reflected in high whole-rock V/*Sc* ratios >12 (Aulbach et al., 2017; Lee et al., 2005). Importantly, at constant temperatures, as the oxidation state increases, the concentration of dissolved sulfide (S^{2-}) in the melt decreases, whereas the dissolved sulfate (SO_4^{2-}) increases as sulfur is oxidized (Richards, 2009; Zhong et al., 2018). Thus, the potential for early precious metal segregation into magmatic sulfide phases is reduced (Richards, 2009). If the sulfide concentration in the melt is reduced, Au and Cu can be concentrated in the volatile-enriched top part of the magma chamber (Müller et al., 2002). Once volatile saturation occurs during secondary boiling, the magma chamber releases pulses of metal- and volatile-enriched melts that can form porphyry Cu-Au mineralization in the upper crust (Müller et al., 2002; Richards, 1995).

High oxidation states of a melt are generally correlated with high magmatic H_2O contents (Williams et al., 2018). Thus, those basalts from oceanic arcs which are most oxidized also have the highest abundances of volatile phases such as magmatic water (Ballhaus, 1993), and Cl and F (Müller et al., 2001).

Within the defined curvilinear fertile arcs, porphyry-related systems are commonly located near the intersections between arc-parallel crustal-scale faults and highly oblique transform or accommodation faults (Figs 12 and 13). Typically, porphyry-related stocks are oxidized magnetite-series I-type intrusions defined by positive "bulls-eye" (e.g., Bajo de la Alumbrera, Argentina: Clark, 2014) or "doughnut"-shaped anomalies in magnetic surveys (e.g., Peschanka, Russia: Chitalin et al., 2021). The magnetic bulls-eye anomalies reflect the biotite-magnetite altered centres of concealed porphyry Cu-Mo deposits (Clark, 2014). By contrast, many gold-rich porphyry Cu deposits hosted by high-K calc-alkaline or shoshonitic intrusions, such as Cadia and Northparkes, Australia, and Mt. Milligan, Canada, are defined by magnetic doughnut anomalies in magnetic surveys (Clark and Schmidt, 2001; Kwan and Müller, 2020). This may be explained by late-stage phyllic alteration that overprints and de-magnetizes the initial biotite-magnetite alteration assemblage via martitization of magnetite to hematite (Kwan and Müller, 2020).

Porphyry clusters typically include both economic porphyry Cu-Au deposits and weakly mineralized and un-economic systems, all of which are genetically associated with similar intrusions derived from the same fractionating magma chamber. This is documented in detail at the Escondida porphyry cluster in northern Chile (Urzua, 2009) and at Oyu Tolgoi, Mongolia (Crane and Kavalieris, 2012). Oyu Tolgoi represents a cluster of seven porphyry Cu-Au systems hosted by quartz-monzonite intrusions that are located above a structurally controlled NE-oriented crustal magma chamber (Crane and Kavalieris, 2012). Importantly, the quartz-monzonite intrusions from the high-grade Hugo Dummett porphyry Cu-Au deposit and the barren Ulan Khud porphyry system are petrographically indistinguishable. Additionally, their whole-rock compositions, including high K and other LILE contents, low HFSE, as well as high Sr/Y and La/Yb ratios, are very similar. Only the mineral chemistry of magmatic zircons and apatites reveals subtle differences between productive and barren intrusions (Loader, 2017; Loader et al., 2017). In other words, while the use of whole-rock geochemistry may be a guide towards fertile intrusive belts through utilization of whole-rock geochemistry and fertility ratios, it cannot assist in the distinction between individual productive and barren intrusions. Geophysical methods are also unable to distinguish between barren and productive porphyry systems as both are defined by similar magnetic and/or IP anomalies. In summary, once a porphyry Cu cluster has been discovered in a fertile intrusive belt, each individual porphyry system of this cluster needs to be evaluated by systematic drilling to define its economic potential.

As suggested by Sillitoe (2010), carbonate host rocks may be important as both restricted reactive host rocks to high-grade Cu-Au or Mo-W skarns and as thick impermeable caps on the magmatic-hydrothermal systems. Iron-rich host rocks may also be important constituents for the genesis of economic porphyry Cu-Au deposits as indicated by the presence of dolerite dykes at Resolution, Arizona (Cooke et al., 2020) and augite-basalt at Oyu Tolgoi, Mongolia (Crane and Kavalieris, 2012). The exposure of lithocaps at the current land surface provides an important indicator that the porphyry-related systems have been uplifted to a suitable level for exploration (Portela et al., 2021).

The large areal extent of porphyry-related systems provides both an advantage and disadvantage in terms of exploration. A major advantage is that it provides a giant alteration and mineralization footprint (Fig. 17) that can be identified through detailed field mapping, ASTER and other remote sensing methods (Alimohammadi et al., 2015; Portela et al., 2021; Pour and Hashim, 2012), and a variety of airborne and ground geophysical surveys.

The disadvantage lies in the difficulty of locating economic mineralization within this broad envelope because, although the systems have broadly the same characteristics in terms of alteration and metal zonation, not all the components shown in Fig. 14 may be present due to erosion or young cover sequences such as ignimbrite flows or gravel plains as in southern Peru and northern Chile (Nalpas et al., 2008). Additionally, each porphyry Cu cluster may have a different geometry depending on the geometry of its underlying magma chamber. These upper crustal parental magma chambers typically are up to 40 km across and up to 3 km thick (Audetat and Simon, 2012; Korges et al., 2020), with individual chambers having circular ellipsoidal (e.g., Bajo de la Alumbrera porphyry Cu-Au deposit, Argentina: Chernicoff et al., 2002) or structurally controlled linear shapes (e.g., Oyu Tolgoi porphyry Cu-Au cluster, Mongolia: Crane and Kavalieris, 2012 or the Llahuin porphyry Au cluster, Chile: Lopez Orrego, 2007). Sillitoe (2010) presents details of these issues in terms of several global porphyry-related systems, and they are beyond the scope of this more general paper.

8. Mineral systems with similar geodynamic and preservation parameters on craton margins

8.1. Introduction

In the discussion above, complete mineral system models are discussed for orogenic gold and porphyry-related deposits. However, from a province scale exploration perspective, the two critical mineral system factors are Geodynamics and Preservation. In the following discussion, deposit classes that have contrasting Fertility and Architecture factors are shown to occupy similar exploration spaces on a continental scale based on Geodynamic and Preservation factors that are specific to craton and thick lithosphere margins where Geodynamic modification promotes mineralization and longevity promotes Preservation.

8.2. Longevity of cratons and their modified margins

Sub-circular Precambrian cratons, normally ~1000 km in diameter, are the foundation blocks of all continents, representing the most stable components of the continental lithosphere in the central portions of tectonic plates. Their longevity is due to their exceptionally deep roots into the asthenosphere, >250 km for some Archean cratons as defined by mantle tomography or satellite gravity, and their temporally variable mineralogical compositions (Griffin et al., 2003; O'Reilly and Griffin, 2010; Vasanthi and Santosh, 2021). These key parameters mean that they represent neu-

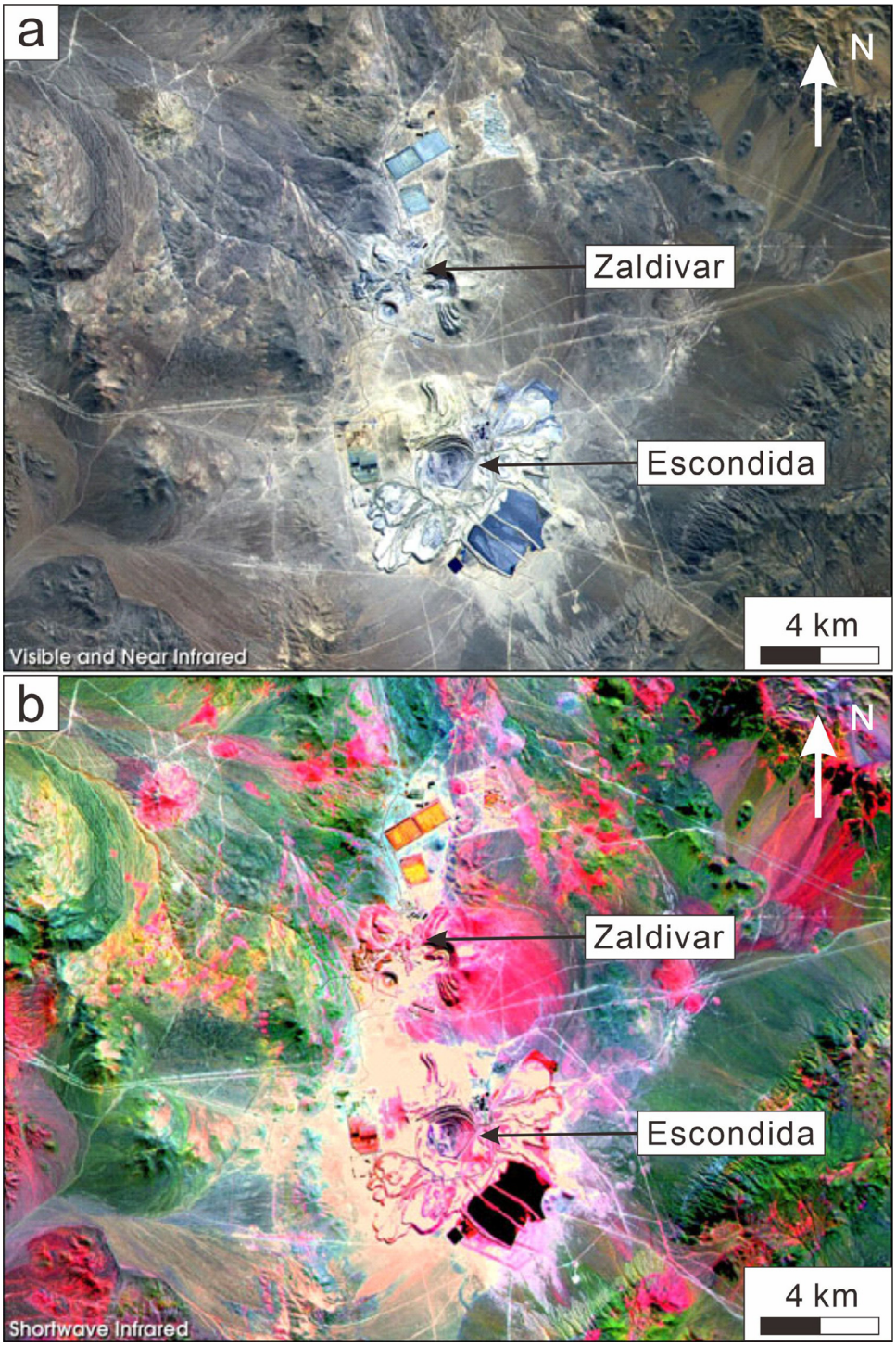

Fig. 17. Advanced Spaceborne Thermal Emission and Reflection Radiometer (ASTER) image of part of the Atacama Desert, Chile, acquired in 2000, showing the giant Escondida-Zaldivar porphyry Cu-Au cluster. Escondida is related geologically to three porphyry bodies intruded along the Chilean West Fissure Fault System. A high-grade supergene cap overlies primary sulfide ore. The top image is a conventional 3–2–1 (near infrared, red, green) RGB composite. The bottom image displays shortwave infrared bands 4–6–8 (1.65 μm, 2.205 μm, 2.33 μm) in RGB, and highlights the different rock types present on the surface, as well as the changes caused by mining. From NASA/GSFC/MITI/ERSDAC/JAROS, and U.S./Japan ASTER Science Team..

tral to buoyant rock masses with low intrinsic isopycnic density that stops them sinking into the asthenosphere and allows them to resist tectonic forces that involve both compression, and resultant uplift, and extension, with rifts generally developing between them rather than through them. However, modification of craton margins is key to the location of a variety of world-class deposits adjacent to them (Groves et al., 2020a).

8.3. Structural and metasomatic modification of craton margins

Although the cratons act as bulwarks that resist deformation relative to rheologically weaker surrounding rock sequences above thinner lithosphere, stress magnitudes and resulting strain gradients are much greater on craton margins than in their interiors where pre-existing weaknesses focus strain (Wang et al., 2017).

Thus, during compression or transpression, external rock sequences may be flattened against the craton margin, be translated by oblique-slip shear movement along the margin, or be thrust above it, providing a range of structural pathways, traps, and caps in terms of the Architecture factors for a variety of mineral systems.

Extensional tectonic events involving rifting also appear to be critical for development of precursor structural geometries that control subsequent magma or hydrothermal fluid flux during later mineralization events (Corti et al., 2013). Extension has the capacity to develop a wide zone of crustal permeability through development of trans-lithosphere faults adjacent to the craton margin, combined with a strong control on sedimentary facies in basins developed on the locally faulted and thinned lithosphere. The Carlin District on the margin of the rifted North American Craton (Cline et al., 2005) is an excellent example.

Widespread heterogeneous metasomatic alteration of mantle lithosphere, particularly on craton margins, has been recognized through the study of the petrology, mineralogy and fluid inclusions within mantle xenoliths brought to upper crustal levels by kimberlites and basaltic magmas (O'Reilly and Griffin, 2013). Such heterogeneous metasomatic alteration may be caused by low-degree partial melts that produced both carbonatite and silicate magmas containing a wide variety of high-density fluids including carbonatitic, hydrosilicic, and saline-brine endmembers (Rosenbaum et al., 1996). The causes may vary from fertilization by low-degree asthenosphere melts, through veining of the lithosphere during plume activity or rifting events, or by fluid-related fertilization during subduction (Litasov et al., 2000; Hughes et al., 2015) which would overprint earlier metasomatic alteration and potentially enhance volatile and metal contents in the mantle lithosphere (Saunders et al., 2018; Wang et al., 2020d).

Importantly, as discussed above for orogenic gold mineral systems, oceanic crust and the overlying sediment wedge will inevitably be subducted below craton margins where devolatilization of the slab can result in extensive upward fluid-flux along slab-mantle boundaries (Peacock et al., 2011, and references therein), into fore-arc or accreting terrane margins, or into the mantle lithosphere (Wyman et al., 2008, 2016, and references therein). Metasomatic fluid thus released can provide ore metals and sulfur via breakdown of pyrite to pyrrhotite (Steadman et al., 2013, and references therein) above about 500^0C, with aqueous fluid, CO_2 and other components released at similar temperatures from breakdown of hydrous silicates and carbonate minerals. Slab devolatilization (Bekaert et al., 2021) and low degrees of partial melting are thus incredibly effective processes for fertilization of mantle lithosphere beneath craton margins during each subduction event that affects them, either directly or indirectly (Castro et al., 2010).

8.4. Magmatic systems derived from metasomatized mantle lithosphere

A wide variety of anomalous magmatic mineral systems that are sited around the margins of cratons and thick lithosphere blocks (Fig. 18) were derived from anomalously abundant metasomatized and fertilized mantle lithosphere along these boundaries (Groves and Santosh, 2021). These include REE-enriched carbonatite-associated Cu-P deposits such as in the Paleoproterozoic Palabora Complex, on the margin of the Kaapvaal Craton in South Africa (Dostal, 2017; Groves and Vielreicher, 2001). There are also carbonatite-associated REE (+/- Nb) deposits such as the giant Mesoproterozoic Bayan Obo deposit on the northern margin of the North China Craton (Fan et al., 2014). This well-researched deposit was formed during a complex magmatic and magmatic-hydrothermal history involving several carbonatite magmas and evolved late fluid phases (Yang et al., 2019). World-wide deposits include Mountain Pass on the margin of the North American Craton (Castor, 2008; Dostal, 2017) and the REE-enriched carbonatites of the Cummins Range Carbonatite Complex at the southern margin of the Kimberley Block, Western Australia (Spandler et al., 2020). The latter are important as there are three periods of Proterozoic alkaline activity spanning 800 million years, implicating repetitive melting of the same underlying metasomatized and fertilized mantle lithosphere whenever the craton margin was extended, as also indicated by Dostal (2017).

Giant Paleoproterozoic Kiruna-type magnetite-apatite deposits are associated with alkaline intrusions derived from metasomatized mantle lithosphere on the margin of the Norbotten Craton (Bauer et al., 2016), with similar Mesoproterozoic deposits at Pea Ridge on the margin of the North American Craton (Alienikoff et al., 2016). In addition, Neoproterozoic lamproite-associated diamond deposits, famous for their rare pink and cognac-brown diamonds (Boxer et al., 2017), are sited at Argyle on the eastern margin of the Kimberley Block, Western Australia.

8.5. Magmatic-hydrothermal systems derived from metasomatized mantle lithosphere

Following supercontinent assembly and during initiation of rifting, magmatic-hydrothermal deposits were formed from hybrid melts derived from metasomatized mantle lithosphere and crustal melting on craton margins. As for the magmatic systems, they owe their preservation, despite their antiquity, to their location within the stable cratons that host them. The most globally widespread and economically important systems are the group of largely Archean to Mesoproterozoic iron-oxide copper-gold (IOCG) deposits (Groves et al., 2010) commonly in breccia pipes (Oliver et al., 2006). There are major clusters at Carajas on the Amazon Craton margin and in South Australia on the Gawler Craton margin, that include the breccia dominated giant Olympic Dam deposit (Ehrig et al., 2017). As discussed in the section above on orogenic gold systems, recent magneto-telluric surveys in the Gawler Craton have shown that narrow low resistivity zones that extend from the ductile-brittle transition in the crust to the surface coincide with the positions of the three main IOCG deposits in the district, particularly the giant Olympic Dam deposit (Heinson et al., 2018). These zones are spatially correlated with narrow regions of low seismic reflectivity in the upper crust with almost transparent deeper lower-crust conductors and are interpreted to represent continental-scale ore fluid pathways with the low resistivity upper crustal zones that project to the IOCG deposits (Fig. 9) termed "Fingers of God" (Robertson and Thiel, 2019). There are obvious implications for detection of deeply derived mineral systems, such as those derived from fertilized mantle lithosphere, during exploration.

Although controversial, some post-collisional or intra-continental porphyry-skarn Cu-Au-W systems, including those of eastern Tibet near the western margin of the Yangtze Craton have also been considered related to reactivation of subduction-modified metasomatized lithosphere. Richards (2009), for example, suggests that the post-collisional porphyry systems are related to fluids derived from melting of such modified lithosphere by post-subduction lithosphere thickening, lithosphere extension, or mantle lithosphere delamination.

Onset of extension and asthenosphere upwelling also facilitated generation of Intrusion-related Gold Deposits (IRGDs) and Carlin-type deposit classes in the back-arc environments adjacent to fragmented craton margins. The hosts for both deposit classes are deformed and metamorphosed continental shelf successions that include both clastic and carbonate units.

The IRGDs (Hart et al., 2002; Lang et al., 2000) represent zoned magmatic-hydrothermal deposits that formed around cupola-like

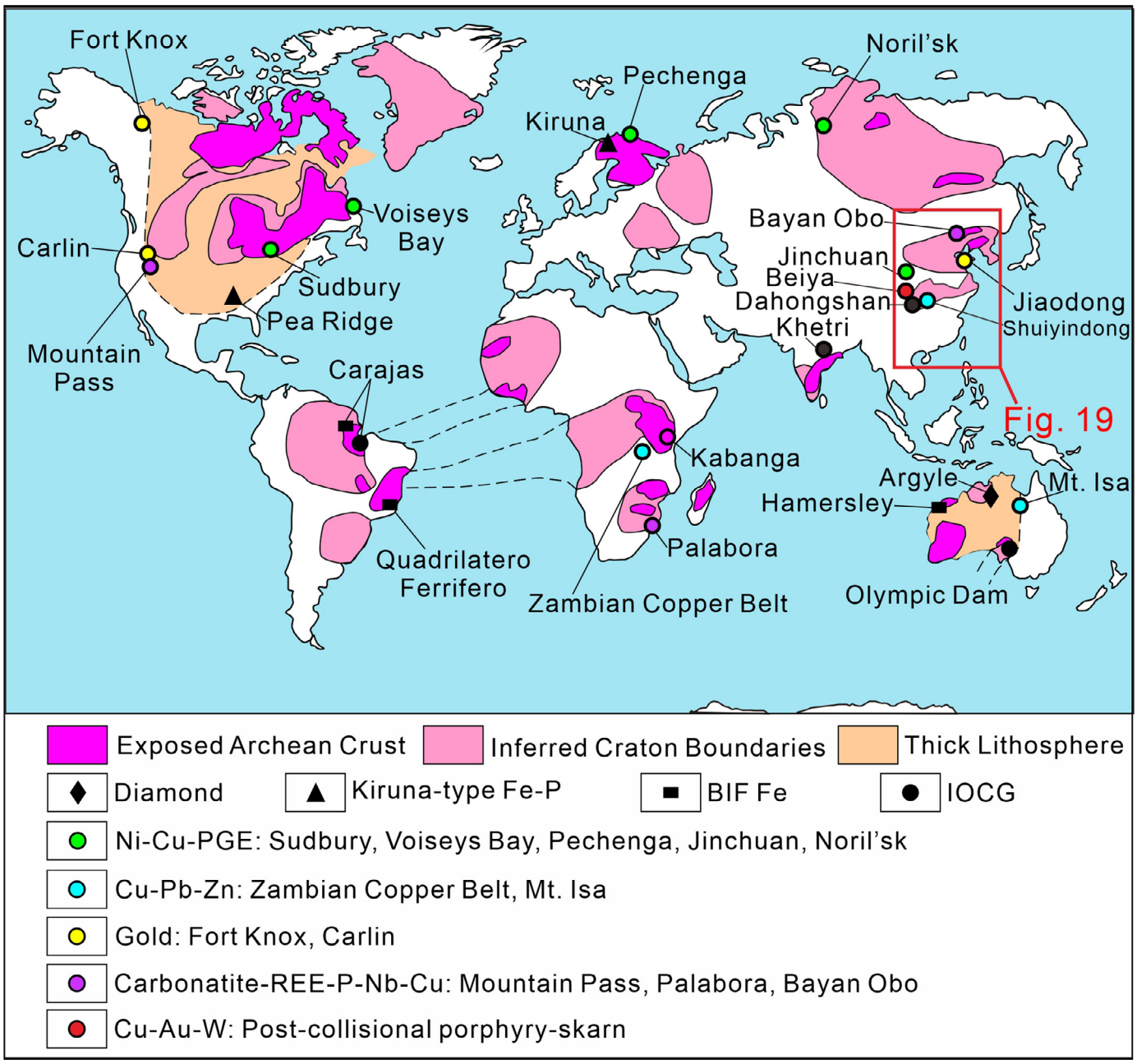

Fig. 18. Global map showing giant to world-class mineral deposits with indirect Geodynamics relationship to subduction sited on craton margins. These margins were selectively mineralized because of their marginal deep fault systems or due to their underlying metasomatized and fertilized mantle lithosphere. Adapted from Groves and Santosh (2021) and Groves et al. (2020b).

protrusions of non-porphyritic, reduced granite intrusions through exsolution of H_2O–CO_2–CH_4 fluids at crustal depths below about 5 km. The related hybrid magmas were generated by partial melting of metasomatized lithosphere to form lamprophyre melts that ponded below the MOHO. These, in turn, caused crustal melting with ore element and volatile transfer across chemical gradients between the two magma types, leading ultimately to gold deposition in extensional vein arrays through fluids liberated from hybrid felsic magmas (Mair et al., 2011).

To the south of the classic Tintina IRGD province of Alaska and Yukon, along the same margin of the North American Craton, is the younger classic Carlin gold province of Nevada (Cline et al., 2005). Auriferous arsenian pyrite provides the ore in replacement bodies within reactive dolomitic units controlled by extensional reactivation of the earlier structural architecture. Although the precise origin of the ore fluids is debated, the driving force for hydrothermal circulation was a similar hybrid magmatic system derived from subduction-related fertilization of underlying lithosphere to that generating the IRGDs (Muntean et al., 2011). Slightly deeper Carlin-type deposits are recorded from the Youjiang Basin in China (Wang and Groves, 2018) where a more distal hybrid magmatic input is implied.

8.6. Hydrothermal systems derived from metasomatized mantle lithosphere

The orogenic gold deposits close to the margins of the North China and Yangtze cratons, particularly those of the Jiaodong Peninsula, are examples of hydrothermal systems derived from fluids sourced via devolatilization of metasomatized mantle litho-

sphere and lacking magmatic input. As they are discussed above in the section on orogenic gold deposits, there is no further discussion here.

8.7. Mineral systems related to craton margin faults and sedimentary basins

Although derived from melting of normal, rather than metasomatized, mantle lithosphere, some mineral systems owe their formation and preservation to the emplacement of parent magmas along craton margins. As noted above, these are the boundaries of greatest rheological contrast and structural weakness in the continents. A key example is provided by largely Precambrian intrusion-related Ni-Cu-PGE deposits which are typically sited within 100 km of craton margins, particularly those of the Superior, Siberia, North China, and Kola-Karelia cratons, as their faulted margins represent the conduits up which the host basic-ultrabasic intrusions are guided (Begg et al., 2010; Maier and Groves, 2011).

Several non-magmatic mineral systems formed on faulted craton margins due to the conjunction of hydrothermal fluid access via the extensive deep fault systems and the presence of both metal reservoir rock units and reactive or permeable host sequences in the continental margin sedimentary successions landward of former subduction zones. This group of mineral systems include Zambian Copperbelt-type Cu-Co deposits (Hitzman et al., 2005) that formed in reduced sedimentary units from fluids enriched in Cu and Co derived from shallow marine sedimentary successions deposited in continental basins that overlie the margins of thick lithosphere and cratons in southern central Africa (Hoggard et al., 2020). Widespread Precambrian iron ores in banded iron formations, where the high-grade iron ores formed by dissolution of silica in the BIFs rather than deposition of iron (Duuring et al., 2018; Evans et al., 2013), also belong to this group.

9. Exploration implications for mineral systems on craton margins

An important question is if this craton association impacts the ground selection process in mineral exploration, arguably the most important decision-making period in an exploration program (Hronsky and Groves, 2008). From a qualitative viewpoint, it clearly does provide new exploration search spaces for a wide variety of disparate mineral systems whose Fertility and Architecture factors vary despite their similar Geodynamic and Preservation factors. Groves and Santosh (2021) point out the many constraints on estimation of exploration-project potential endowment (Kreuzer et al., 2008). They conclude that, for the mineral systems discussed above, most deposits would lie within ~10%, with all lying within ~20% of the total area of continental crust globally. Similarly, Hoggard et al. (2020) calculate that ~35% of the continental crust would include all giant sediment-hosted Pb-Zn-Cu deposits for a 200 km buffer around thick lithosphere margins.

This may not appear to be a substantial advantage in exploration targeting. However, Groves and Santosh (2021) show that these areas could be significantly reduced for exploration because many of the deposit classes in craton-proximal mineral systems have distinctive geophysical signatures, particularly in terms of magnetic and/or gravity signals, but also TEM and IP signals for sulfide-rich deposits.

A spectacular example of the endowment of craton margins for a wide diversity of deposit classes is provided in eastern China by the occurrence of 66 world-class to giant deposits within ~ 100 km of the margins of the North China and Yangtze cratons (Fig. 19:Yang et al., 2021).

Another excellent example of the prospectivity of craton margins is provided by the margins of the Yilgarn Craton in Western Australia. Here, three of the four most recent major discoveries have been made within ~ 50 km of the craton margin: the Tropicana orogenic gold deposit (> 240 tonnes gold: Doyle et al., 2017), Nova-Bollinger intrusion-hosted Ni-Cu deposit (14.3 Mt @ 2.3% Ni, 0.9% Cu: Parker et al., 2017) and most recent Julimar intrusion hosted PGE-Ni-Cu deposit with Pd grades equivalent to those of the giant Noril'sk-Talnakh deposits of Russia (Chalice Gold Mines Ltd website). Previously discovered deposits within ~100 km of the Yilgarn Craton margin include the giant Boddington Au (Cu, Mo) deposit (Turner et al., 2020) and the giant Greenbushes Li-Ta-Sn deposit (Partington, 2017).

10. Conclusions

Mineral systems provide a logical and hierarchical mechanism to integrate information over a range of time and terrane scales using the broad critical components of Geodynamics (tectonic setting), Fertility (source of ore and hydrothermal fluid components), Architecture (fluid plumbing systems) and Preservation (degree of post-ore uplift and erosion). Although their adoption in published economic geology literature appears limited, the value of such mineral systems for single deposit classes, using orogenic gold as an example, and closely related deposit groups, using porphyry-high-sulfidation-skarn Cu-Au-Mo systems as an example, is demonstrated above. The value of grouping disparate deposit classes based on similarities of their Geodynamics and Preservation parameters is demonstrated by the siting of numerous, not normally grouped, deposit classes on the margins of cratons and blocks with thick mantle lithosphere. Consideration as mineral systems provides a useful way of "seeing the wood for the trees" and defining universally applicable genetic models for deposit classes. It also allows focus on the critical measurable parameters that aid exploration to the exclusion of small-scale information that may only be uniquely applicable to the specific deposit from which it was derived.

Application to orogenic gold deposits illustrates the value of a mineral system model for a single deposit class under the premise that their genesis be explained in terms of a universal global model rather than a series of disparate local or time-dependent models. For a coherent mineral system, there are only two realistic sources of fluid and gold to generate orogenic gold deposits over vertical crustal depths of 2–20 km, based on their late-orogenic, syn-mineralization Geodynamic settings in convergent margins. These Fertility sources must either be devolatilization of a subducted oceanic slab with its overlying gold-bearing sulfide-rich sedimentary package, or release from mantle lithosphere that was metasomatized and fertilized during a previous subduction event, particularly adjacent to craton margins. In terms of the Architecture parameter, over-pressured sub-crustal ore fluids were channeled up lithosphere-scale shear zones to a variety of repetitive combined structural and lithological trap sites where gold was deposited below low-permeability caps. The late-orogenic timing and deep crustal level of formation dictated a high Preservation factor, with orogenic gold deposits recorded from the Mesoarchean to the Cenozoic. The orogenic gold mineral system can be applied to conceptual exploration using the critical gold mineralization parameters in the system. These parameters dictate, among others, that the structures controlling ore fluid advection must be lithosphere-scale, not simply crustal scale, faults that can be identified in magneto-telluric surveys, and that amphibolite-facies metamorphic domains are prospective exploration search spaces.

The porphyry-high sulfidation-skarn deposit group is an example where the mineral system comprises several individually recognized Cu-Au, Cu-Mo, and Zn-Pb-Au-Ag deposit classes that

Fig. 19. Tectonic framework of Eastern China showing 66 world-class to giant mineral deposits within ~100 km of the margins of the North China and Yangtze cratons: compiled from multiple sources, mainly within Chang and Goldfarb (2019). Gold deposits in Qinling-Dabie Orogen classified according to Goldfarb et al. (2019). From Yang et al. (2021).

are commonly spatially and temporally associated. These occur in elongate, curvilinear volcanic, continental, island, and post-collisional arcs, particularly those underlain by metasomatized mantle lithosphere, where they are controlled in terms of Geodynamics and province-scale Architecture by intersection of arc-parallel continental-scale faults by oblique crustal-scale accommodation fault structures. Fertility of the arcs is defined by geochemical compositions of volcanic components that reflect residence and replenishment of oxidized and H_2O-rich source magmas in upper crustal magma chambers. In terms of district-scale Architecture, the porphyry-related systems are sited in and above large non- or sparsely porphyritic batholiths, and hosted by finger-shaped composite porphyritic plugs, or more rarely, dykes. The mineral systems are represented by vertically and laterally zoned shells that include orebodies, alteration envelopes, and metal ratios developed from long-lived, originally highly saline and low pH, evolving magmatic-hydrothermal fluids exsolved from the fertile porphyry intrusions. Preservation potential is limited because of high uplift and erosion rates in the host arcs, especially island arcs, with most deposits restricted to the Cenozoic, although there are Mesozoic

examples in post-collisional arcs, and even rare Precambrian examples. At the district scale, the preservation of lithocaps identifies systems that are at a suitable exhumation level for exploration, with a range of mapping, remote sensing, and geophysical methodologies applicable to the detection of critical responses from the extensive porphyry-related mineral system, although drilling is ultimately required to establish whether the systems are economically viable.

The value of considering disparate deposit classes in terms of one or more common mineral system parameters is shown by analysis of deposits on craton and thick lithosphere margins. These represent a specific Geodynamic setting with a high Preservation factor for an incredibly large range of normally unrelated deposit classes enriched in Ag, Au, Bi, Co, Cu, Fe, Mo, Ni, P, Pb, PGE, REE, Sb, Sn, Te, W, and Zn, and including diamonds. These deposit classes are sited within ~100 km of the margins due to the requirement of a source derived from metasomatized and fertilized mantle lithosphere or due to development of lithosphere-scale fault arrays and/or fertile marginal basins on these margins. Thus, although Fertility and Architecture components vary widely between component mineral systems, the combined Geodynamic and Preservation factors provide specific restricted exploration search spaces for a variety of deposit classes. This is shown in spectacular fashion for the North China and Yangtze cratons in eastern China where 66 giant or world class deposits of diverse type are sited within ~100 km of their margins. In Western Australia, several of the most recent major discoveries of world-class gold, Ni-Cu, and Pd-Pt-Cu-Ni-Co deposits have been made on the margins of the Yilgarn Craton.

Declaration of Competing Interest

The authors declare that they have no known competing financial interests or personal relationships that could have appeared to influence the work reported in this paper.

Acknowledgments

This paper was inspired by the discussion of development of The Critical Minerals Mapping Initiative (CMMI) by Karen Kelley, David Huston, and Jan Peter (2021). Inspiration for some of the concepts presented above was also provided from discussions with (in alphabetical order) Graham Begg, Frank Bierlein, Rich Goldfarb, Jon Hronsky, and Derek Wyman. M. Santosh was supported for his research by China University of Geosciences Beijing, China and University of Adelaide, Australia. Funding for the research on which this paper was based includes the National Key Research Program of China (Grant Nos. 2019YFA0708603, 2016YFC0600307), the National Natural Science Foundation of China (Grant Nos. 41230311, 41572069), the 111 Project of the Ministry of Science and Technology (BP0719021), the MOST Special Fund from the State Key Laboratory of Geological Processes and Mineral Resources, China University of Geosciences (Grant No. MSFGPMR201804).

References

Alimohammadi, M., Alirezaei, S., Kontak, D.J., 2015. Application of ASTER data for exploration of porphyry copper deposits: a case study of Daraloo-Sameshk area, southern part of the Kerman copper belt, Iran. Ore Geol. Rev. 70, 290–304.
Audetat, A., Simon, A.C., 2012. Magmatic controls on porphyry copper genesis. Econ. Geol. Special Publ. 16, 553–572.
Audetat, A., Li, W., 2017. The genesis of Climax-type porphyry Mo deposits: insights from fluid inclusions and melt inclusions. Ore Geol. Rev. 88, 436–460.
Aulbach, S., Woodland, A.B., Vasylyev, P., Galvez, M.E., Viljoen, K.S., 2017. Effects of low-pressure igneous processes and subduction on $Fe^{3+}/Fe\Sigma$ and redox state of mantle eclogites from Lace (Kaapvaal Craton). Earth Planet. Sci. Lett. 474, 283–295.
Ballhaus, C., 1993. Redox states of lithospheric and asthenospheric upper mantle. Contrib. Mineral. Petrol. 114, 331–348.
Bao, X.S., Yang, L.Q., He, W.Y., Gao, X., 2018. Importance of magmatic water content and oxidation state for porphyry-style Au mineralization: an example from the giant Beiya Au deposit, SW China. Minerals 8, 441.
Barley, M.E., 1982. Porphyry-style mineralization associated with early Archean calc-alkaline igneous activity, eastern Pilbara, Western Australia. Econ. Geol. 77, 1230–1236.
Bauer, T.E., Anderson, J.B.H., Sarius, Z., Lund, C., Kearny, T., 2016. Structural controls on the setting, shape, and hydrothermal alteration of the Malmberget iron-oxide-apatite deposit, northern Sweden. Econ. Geol. 113, 377–395.
Begg, G.C., Hronsky, J.M.A., Arndt, N.T., Griffin, W.L., O'Reilly, S.Y., Hayward, N., 2010. Lithospheric, cratonic and geodynamic setting of Ni-Cu-PGE sulfide deposits. Econ. Geol. 105, 1057–1070.
Bekaert, D.V., Turner, S.J., Broadley, M.W., Barnes, J.D., Halldórsson, S.A., Labidi, J., Wade, J., Walowski, K.J., Barry, P.H., 2021. Subduction-driven volatile recycling: a global mass balance. Annu. Rev. Earth Planet. Sci. 49, 37–70.
Bierlein, F.P., Groves, D.I., Goldfarb, R.J., Dube, B., 2006a. Lithospheric controls on the formation of giant orogenic gold deposits. Miner. Depos. 40, 874–886.
Bierlein, F.P., Murphy, F.C., Weinberg, R., Lees, T., 2006b. Distribution of orogenic gold deposits in relation to fault zones and gravity gradients: targeting tools applied to the Eastern Goldfields, Yilgarn Craton, Western Australia. Miner. Depos. 41, 107–126.
Bierlein, F.P., Pisarevsky, S., 2008. Plume-related oceanic plateaus as a potential source of gold mineralization. Econ. Geol. 103, 425–430.
Blevin, P.L., 2002. The petrographic and compositional character of variably K-enriched magmatic suites associated with Ordovician porphyry Cu-Au mineralization in the Lachlan Fold Belt, Australia. Miner. Depos. 37, 87–99.
Bouchot, V., Ledru, P., Lerouge, C., Lescuyer, J.L., Milesi, J.P., 2005. Late Variscan mineralizing systems related to orogenic processes: the French Massif Central. Ore Geol. Rev. 27, 169–197.
Boxer, G.I., Jaques, A.l., Rayner, N.J., 2017. Argyle (AK1) diamond deposit. In: Phillips, G.N. (Ed.), Australian Ore Deposits. Monograph 32. Australasian Institute of Mining and Metallurgy Melbourne, pp. 527–531.
Bruce, M., Kreuzer, O., Wilde, A., Buckingham, A., Butera, K., Bierlein, F., 2020. Unconformity-type uranium systems: a comparative review and predictive modelling of critical genetic factors. Minerals 10, 738.
Cabrera, J., 2011. Estudio petrografico y petrológico de los pórfidos alimentadores del distrito mina Radomiro Tomic, II Region, Chile. Universidad de Concepcion, Chile, p. 179 Unpubl. MSc Thesis.
Cao, M.J., Qin, K.Z., Li, G.M., Evans, N.J., McInnes, B.I.A., Li, J.X., Zhao, J.X., 2018. Oxidation state inherited from the magma source and implications for mineralization: late-Jurassic to Early-Cretaceous granitoids, central Lhasa subterrane, Tibet. Miner. Depos. 53, 299–309.
Castor, S.B., 2008. Rare earth deposits of North America. Resour. Geol. 58, 337–347.
Castro, A., Gerya, T., García-Casco, A., Fernández, C., Díaz-Alvarado, J., Moreno-Ventas, I., Löw, I., 2010. Melting relations of MORB–sediment mélanges in underplated mantle wedge plumes; implications for the origin of Cordilleran-type batholiths. J. Petrol. 51, 1267–1295.
Chang, Z., & Goldfarb, R.J. (2019).Eds, Mineral Deposits of China: An Introduction: Society of Economic Geologists Special Publication 22, 1–11.
Chen, Y.J., Pirajno, F., Qi, J.P., 2008. The Shanggong gold deposit, Eastern Qinling Orogen, China— Isotope geochemistry and implication for ore genesis. J. Asian Earth Sci. 33, 252–266.
Chernicoff, C.J., Richards, J.P., Zappettini, E.O., 2002. Crustal lineament control on magmatism and mineralization in northwestern Argentina: geological, geophysical, and remote sensing evidence. Ore Geol. Rev. 21, 127–155.
Chitalin, A.F., Baksheev, I.A., Nikolaev, Y.N., Djedjeya, G.T., Khabibullina, Y.N., Müller, D., 2021. Porphyry Cu–Au+Mo mineralization hosted by potassic igneous rocks: implications from the giant Peschanka porphyry deposit. Baimka Trend (North-East Siberia, Russia). Geological Society. Special Publication 513, London.
Clark, D.A., 2014. Magnetic effects of hydrothermal alteration in porphyry copper and iron-oxide copper–gold systems: a review. Tectonophysics 625, 46–65.
Clark, K.F., Foster, C.T., Damon, P.E., 1982. Cenozoic mineral deposits and subduction-related magmatic arcs in Mexico. GSA Bull. 93, 533–544.
Clark, D.A., .& Schmidt, P.W. (.2001). Petrophysical properties of the goonumbla volcanic complex, NSW: implications for magnetic and gravity signatures of porphyry Cu-Au mineralisation. ASEG Extended Abstracts 2001, 1–4.
Cline, J.S., Hofstra, A.H., Muntean, J.L., Tosdal, R.M., Hickey, K.A., 2005. Carlin-type gold deposits in Nevada: critical geologic characteristics and viable models. In: Proceedings of the Economic Geology 100th Anniversary Volume, pp. 451–484.
Cocker, H.A., Valente, D.L., Park, J.W., Campbell, I.H., 2016. Using platinum group elements to identify sulfide saturation in a porphyry Cu system: the El Abra porphyry Cu deposit, northern Chile. J. Petrol. 56, 2491–2514.
Colvine, A.C., Andrews, A.J., Cherry, M.E., Durocher, M.E., Fyon, J.A., Lavigne, M.J., Macdonald, A.J., Marmont, S., Poulsen, K.H., Springer, J.S., Troop, D.G., 1984. An integrated model for the origin of Archean lode-gold deposits. Ont. Geol. Surv. Open-File Report 5524, 98.
Cooke, D.R., Wilkinson, J.J., Baker, M., Agnew, P., Phillips, J., Chang, Z., Chen, H., Wilkinson, C.C., Inglis, S., Hollings, P., Zhang, L., Gemmell, J.B., White, N.C., Danyushevsky, L., Martin, H., 2020. Using mineral chemistry to aid exploration: a case study from the Resolution porphyry Cu-Mo deposit, Arizona. Econ. Geol. 115, 813–840.

Corbett, G.J., Leach, T.M., 1998. In: Southwest Pacific Rim Gold-Copper Systems: Structure, Alteration and Mineralization, 6. Society of Economic Geologists Special Publication, p. 240.
Corti, G., Iandelli, I., Cerca, M., 2013. Experimental modelling of rifting at craton margins. Geosphere 9, 138–154.
Cox, S.F., 2016. Injection-driven swarm seismicity and permeability enhancement: implications for the dynamics of hydrothermal ore systems in high fluid-flux, over-pressured faulting regimes-an invited paper. Econ. Geol. 111, 559–588.
Crane, D., Kavalieris, I., 2012. In: Geologic Overview of the Oyu Tolgoi Porphyry Cu-Au-Mo Deposits, Mongolia, 16. Economic Geology Special Publication, pp. 187–213.
Deng, J., Yang, L.Q., Groves, D.I., Zhang, L., Qiu, K.F., Wang, Q.F., 2020a. An integrated mineral system model for the gold deposits of the giant Jiaodong Province, eastern China. Earth Sci. Rev. 208, 103274.
Deng, J., Wang, Q.F., Santosh, M., Liu, X., Liang, Y., Yang, L.Q., Zhao, R., Yang, L., 2020b. Remobilization of metasomatized mantle lithosphere: a new model for the Jiaodong gold province, eastern China. Miner. Depos. 55, 257–274.
Deng, J., Qiu, K.F., Wang, Q.F., Goldfarb, R.J., Yang, L.Q., Zi, J.W., Geng, J.Z., Ma, Y., 2020c. *In situ* dating of hydrothermal monazite and implications for the geodynamic controls on ore formation in the Jiaodong gold province, eastern China. Econ. Geol. 115, 671–685.
Deng, J., Wang, Q.F., Gao, L., He, W.Y., Yang, Z.Y., Zhang, S.H., Chang, L.J., Li, G.J., Sun, X., Zhou, D.Q., 2021. Differential crustal rotation and its control on giant ore clusters along the eastern margin of Tibet. Geology 49, 428–432.
Dentith, M.D., Aitkin, A., Evans, S., Joly, A., 2013. Regional targeting for gold and nickel deposits using crustal electrical conductivity variations determined using the magnetotelluric method. Aust. Soc. Explor. Geophys. Ext. Abstr. 124, 1–4.
Dilles, J.H., Kent, A.J.R., Wooden, J.L., Tosdal, R.M., Koleszar, A., Lee, R.G., Farmer, L.P., 2015. Zircon compositional evidence for sulfur-degassing from ore-forming arc magmas. Econ. Geol. 110, 241–251.
Dostal, J., 2017. Rare earth element deposits of alkaline igneous rocks. Resources 6, 34.
Doyle, M.G., Catto, B., Gibbs, D., Kent, M., Savage, J., 2017. Tropicana gold deposit. In: Phillips, G.N. (Ed.), Australian Ore Deposits. Monograph 32. Australasian Institute of Mining and Metallurgy Melbourne, pp. 299–306.
Duuring, P., Hagemann, S.G., Banks, D.A., Schindler, C., 2018. A synvolcanic origin for magnetite-rich orebodies hosted by BIF in the Weld Range District, Western Australia. Ore Geol. Rev. 93, 211–254.
Ehrig, K., Kamenetsky, V.S., McPhie, J., Cook, N.J., Ciobanu, C.L., 2017. Olympic Dam iron oxide Cu-U-Au-Ag deposit. In: Phillips, G.N. (Ed.), Australian Ore Deposits. Monograph 32. Australasian Institute of Mining and Metallurgy Melbourne, pp. 601–610.
Espurt, N., Funicielo, F., Martinod, J., Guillaume, B., Regard, V., Faccenna, C., Brusset, S., 2008. Flat subduction dynamics and deformation of the South American Plate: insights from analog modelling. Tectonics 27 TC 3011.
Evans, K.A., McCuaig, T.C., Leach, D., Angerer, T., Hagemann, S.G., 2013. Banded iron formation to iron ore: a record of the evolution of Earth environments? Geology 41, 99–102.
Fan, H.R., Hu, F.F., Yang, K.F., Pirajno, F., Liu, X., Wang, K.Y., 2014. Integrated U-Pb and Sm-Nd geochronology for a REE-rich carbonatite dyke at the giant Bayan Obo REE deposit, Northern China. Ore Geol. Rev. 63, 510–519.
Fox, N., Cooke, D.R., Harris, A.C., Collett, D., Eastwood, G., 2015. Porphyry Au-Cu mineralization controlled by reactivation of an arc-transverse volcano-sedimentary subbasin. Geology 43, 811–814.
Fu, Y., Sun, X., Zhou, H., Lin, H., Jiang, L., Yang, T., 2017. In-situ LA-ICP-MS trace elements analysis of scheelites from the giant Beiya gold–polymetallic deposit in Yunnan Province, Southwest China and its metallogenic implications. Ore Geol. Rev. 80, 828–837.
Garwin, S., Hall, R., Watanabe, Y., 2005. Tectonic setting, geology, and gold and copper mineralization in Cenozoic magmatic arcs of southeast Asia and the west Pacific. In: Proceedings of the Economic Geology 100th Anniversary Volume, pp. 891–930.
Gebre-Mariam, M., Hagemann, S.G., Groves, D.I., 1995. A classification scheme for epigenetic Archaean lode-gold deposits. Miner. Depos. 30, 408–410.
Geological Survey of Western Australia, 2011. Southern Cross Magnetotelluric (MT) Survey. Geological Survey of Western Australia website.
Goldfarb, R.J., Baker, T., Dubé, B., Groves, D.I., Hart, C.J.R., Gosselin, P., 2005. Distribution, character, and genesis of gold deposits in metamorphic terranes. In: Proceedings of the Economic Geology 100th Anniversary Volume, pp. 407–450.
Goldfarb, R.J., Groves, D.I., 2015. Orogenic gold: common vs evolving fluid and metal sources through time. Lithos 223, 2–26.
Goldfarb, R.J., Groves, D.I., Gardoll, S., 2001. Orogenic gold and geologic time; a global synthesis. Ore Geol. Rev. 18, 1–75.
Goldfarb, R.J., Leach, D.L., Pickthorn, W.J., Paterson, C.J., 1988. Origin of lode–gold deposits of the Juneau gold deposit, southeast Alaska. Geology 16, 440–443.
Goldfarb, R.J., Qiu, K.F., Deng, J., Chen, Y.J., Yang, L.Q., 2019. In: Orogenic Gold Deposits of China, 22. Society of Economic Geologists Special Publication, pp. 263–324.
Goldfarb, R.J., Santosh, M., 2014. The dilemma of the Jiaodong gold deposits: are they unique? Geosci. Front. 5, 139–153.
Goldfarb, R.J., Taylor, R.D., Collins, G.S., Goryachev, N.A., Orlandini, O.F., 2014. Phanerozoic continental growth and gold metallogeny of Asia. Gondwana Res. 25, 48–102.
Gow, P.A., Walshe, J.L., 2005. The Role of preexisting geologic architecture in the formation of giant porphyry-related Cu ± Au deposits: examples from New Guinea and Chile. Econ. Geol. 100, 819–833.
Griffin, W.L., Begg, G.C., O'Reilly, S.Y., 2013. Continental root control on the genesis of magmatic ore deposits. Nat. Geosci. 6, 905–910.
Griffin, W.L., O'Reilly, S.Y., Abe, N., Aulbach, S., Davies, R.M., Pearson, M.J., Doyle, B.J., Kivi, K., 2003. The origin and evolution of Archean lithospheric mantle. Precambrian Res. 127, 19–41.
Griffin, W.L., Zhang, A.D., O'Reilly, S.Y., Ryan, C.G., 1998. Phanerozoic evolution of the lithosphere beneath the Sino-Korean Craton. In: Mantle Dynamics and Plate Interactions in East Asia, 27, pp. 107–126.
Groves, D.I., 1993. The crustal continuum model for late-Archaean lode gold deposits of the Yilgarn block, Western Australia. Miner. Depos. 28, 366–374.
Groves, D.I., Bierlein, F.P., Meinert, L.A., Hitzman, M.W., 2010. Iron-oxide copper-gold (IOCG) deposits through Earth history: implications for origin, lithospheric setting and distinction from other epigenetic iron oxide deposits. Econ. Geol. 105, 641–654.
Groves, D.I., Condie, K.C., Goldfarb, R.J., Hronsky, J.M.A., Vielreicher, R.M., 2005a. Secular changes in global tectonic processes and their influence on the temporal distribution of gold-bearing mineral deposits. In: Proceedings of the Economic Geology 100th Anniversary Volume, pp. 203–224.
Groves, D.I., Goldfarb, R.J., Gebre-Mariam, M., Hagemann, S.G., Robert, F., 1998. Orogenic gold deposits–a proposed classification in the context of their crustal distribution and relationship to other gold deposit types. Ore Geol. Rev. 13, 7–27.
Groves, D.I., Goldfarb, R.J., Knox-Robinson, C.M., Ojala, J., Gardoll, S., Yun, G., Holyland, P., 2000. Late-kinematic timing of orogenic gold deposits and its significance for computer-based exploration techniques with emphasis on the Yilgarn block, Western Australia. Ore Geol. Rev. 17, 1–38.
Groves, D.I., Goldfarb, R.J., Robert, F., Hart, C.J.R., 2003. Gold deposits in metamorphic belts: overview of current understanding, outstanding problems, future research, and exploration significance. Econ. Geol. 98, 1–29.
Groves, D.I., Phillips, G.N., Ho, S.E., Houstoun, S.M., Standing, C.A., 1987. Craton-scale distribution of Archean greenstone gold deposits—Predictive capacity of the metamorphic model. Econ. Geol. 82, 2045–2058.
Groves, D.I., Santosh, M., 2015. Province-scale commonalities of some world-class gold deposits: implications for mineral exploration. Geosci. Front. 6, 389–399.
Groves, D.I., Santosh, M., 2016. The giant Jiaodong gold province: the key to a unified model for orogenic gold deposits? Geosci. Front. 7, 409–418.
Groves, D.I., Santosh, M., 2021. Craton and thick lithosphere margins: the sites of giant mineral deposits and mineral provinces. Gondwana Res. doi:10.1016/j.gr.2020.06.008.
Groves, D.I., Santosh, M., Zhang, L., 2020a. A scale-integrated exploration model for orogenic gold deposits based on a mineral system approach. Geosci. Front. 11, 719–738.
Groves, D.I., Santosh, M., Deng, J., Wang, Q.F., Yang, L.Q., Zhang, L., 2020b. A holistic model for the origin of orogenic gold deposits and its implications for exploration. Miner. Depos. 55, 275–292.
Groves, D.I., Santosh, M., Goldfarb, R.J., Zhang, L., 2018. Structural geometry of orogenic gold deposits: implications for exploration of world-class and giant deposits. Geosci. Front. 9, 1163–1177.
Groves, D.I., Vielreicher, N.M., 2001. The Phalabowra (Palabora) carbonatite-related magnetite—Copper sulfide deposit, South Africa: the missing proximal end-member of the Fe-oxide copper-gold-REE deposit group? Miner. Depos. 36, 189–194.
Groves, D.I., .Vielreicher, R.M., .Goldfarb, R.J., .& Condie, K.C. (2005b). Controls on the heterogeneous distribution of mineral deposits through time. In: I., McDonald, A. J., Boyce, I. B., Butler, R. J., Herrington, & D. A., Polya (Eds). Mineral Deposits and Earth Evolution. Geological Society of London Special Publication 248, 71–102.
Hagemann, S.G., Lisitsin, V.A., Huston, D.L., 2016. Mineral system analysis: quo Vadis. Ore Geol. Rev. 76, 504–522.
Halter, W.E., Pettke, T., Heinrich, C.A., 2002. The origin of Cu/Au ratios in porphyry type ore deposits. Science 296, 1844–1846.
Halley, S., 2020. Mapping magmatic and hydrothermal processes from routine exploration geochemical analyses. Econ. Geol. 115, 489–503.
Hao, H., Campbell, I.H., Park, J.W., Cooke, D.R., 2017. Platinum-group element geochemistry used to determine Cu and Au fertility in the Northparkes igneous suites, New South Wales, Australia. Geochim. Cosmochim. 216, 372–392.
Hart, C.J.R., McCoy, D., Goldfarb, R.J., Smith, M., Roberts, P., Hulstein, R., Bakke, A.A., Bundtzen, T.K., 2002. In: Geology, Exploration and Discovery in the Tintina Gold Province, Alaska and Yukon, 9. Society of Economic Geologists Special Publication, pp. 241–274.
Haschke, J.W., Siebel, W., Günther, A., Scheuber, E., 2002. Repeated crustal thickening and recycling during the Andean orogeny in north Chile (21°-26°S). J. Geol. Res. 107 6-1–6-18.
Hattori, K.H., Keith, J.D., 2001. Contribution of mafic melt to porphyry copper mineralization: evidence from Mount Pinatubo, Philippines, and Bingham Canyon, Utah, USA. Miner. Depos. 36, 799–806.
Hayes, G.P., Moore, G.L., Portner, D.E., Hearne, M., Flamme, H., Furtney, M., Smoczyk, G.M., 2018. Slab2, a comprehensive subduction zone geometry model. Science 362, 58–61.
Hedenquist, J.W., Harris, M., Camus, F., 2012. In: Geology and Genesis of Major Copper Deposits and Districts of the World: a Tribute to Richard H. Sillitoe, 16. Society of Economic Geologists Special Publication, pp. 1–618.
Heinrich, C.A., 2005. The physical and chemical evolution of low-salinity magmatic fluids at the porphyry to epithermal transition: a thermodynamic study. Miner. Depos. 39, 864–889.
Heinson, G., Didana, Y., Soeffky, P., Thiel, S., Wise, T., 2018. The crustal geophysical signature of a world-class magmatic mineral system. Nat. Sci. Rep. 8, 10608.

Hitzman, M.W., Kirkham, R., Broughton, D., Thorson, J., Selley, D., 2005. The sediment-hosted stratiform copper ore system. In: Proceedings of the Economic Geology 100th Anniversary Volume, pp. 609–642.
Hollings, P., Cooke, D., Clark, A., 2005. Regional geochemistry of Tertiary igneous rocks in central Chile: implications for the geodynamic environment of giant porphyry copper and epithermal gold mineralization. Econ. Geol. 100, 887–904.
Hronsky, J.M.A., 2011. Self-organized critical systems and ore formation: the key to spatial targeting? Soc. Econ. Geol. Newsl. 84, 14–16.
Hronsky, J.M.A., 2020. Deposit-scale structural controls on orogenic gold deposits: an integrated, physical process-based hypothesis and practical targeting implications. Miner. Depos. 55, 197–216.
Hronsky, J.M.A., Groves, D.I., 2008. The science of targeting: definition, strategies, targeting and performance measurement. Aust. J. Earth Sci. 55, 3–12.
Hronsky, J.M.A., Groves, D.I., Loucks, R.R., Begg, G.C., 2012. A unified model for gold mineralisation in accretionary orogens and implications for regional-scale exploration targeting methods. Miner. Depos. 47, 339–358.
Huang, W., Liang, H., Wu, L., Wu, J., Li, J., Bao, Z., 2018. The relation between Cu/Au ratio and formation depth of porphyry-style Cu–Au ± Mo deposits. Ore Geol. Rev. 102, 351–367.
Hughes, H.S.R., McDonald, I., Faithfull, J.W., Upton, B.G.J., Downes, H., 2015. Trace-element abundances in the shallow lithospheric mantle of the North American Craton margin: implication for melting and metasomatism beneath Northern Scotland. Mineral. Mag. 79, 877–907.
Huston, D.L., Mernagh, T.P., Hagemann, S.G., Doublier, M.P., Fiorentini, M., Champion, D.C., Jaques, A.L., Czarnota, K., Cayley, R., Bastrakov, R.S., 2016. Tectono-metallogenic systems-The place of mineral systems within tectonic evolution, with an emphasis on Australian examples. Ore Geol. Rev. 76, 168–210.
Hyndman, R.D., McCrory, P.A., Wech, A., Kao, H., Ague, J., 2015. Cascadia subducting plate fluids channeled to forearc mantle corner: ETS and silica deposition. J. Geophys. Res. Solid Earth 120, 4344–4358.
Ishihara, S., Chappell, B.W., 2010. Petrochemistry of I-type magnetite-series granitoids of northern Chile, Highland Valley, southern B.C., Canada, Erdenet mine, Mongolia, Dexing mine, China, Medet mine, Bulgaria, and Ani mine, Japan. Bull. Geol. Surv. Jpn. 61, 383–415.
Isozaki, Y., Aoki, K., Nakama, T., Yanai, S., 2010. New insight into a subduction-related orogen: a reappraisal of the geotectonic framework and evolution of the Japanese Island. Gondwana Res. 18, 82–105.
Jamali, H., 2017. The behaviour of rare-earth elements, zirconium and hafnium during magma evolution and their application in determining mineralized magmatic suites in subduction zones: constraints from the Cenozoic belts of Iran. Ore Geol. Rev. 81, 270–279.
Jankovic, S., 1977. The copper deposits and geotectonic setting of the Thethyan Eurasian Metallogenic Belt. Miner. Depos. 12, 37–47.
Katayama, I., Terada, T., Okazaki, K., Tanikawa, W., 2012. Episodic tremor and slow slip potentially linked to permeability contrasts at the Moho. Nat. Geosci. 5, 731–734.
Kawai, K., Tsuchiya, T., Tsuchiya, J., Maruyama, S., 2009. Lost primordial continents. Gondwana Res. 16, 581–586.
Kay, S.M., Mpodozis, C., Tittler, A., Cornejo, P., 1994. Tertiary magmatic evolution of the Maricunga mineral belt in Chile. Int. Geol. Rev. 36, 1079–1112.
Kelley, K.D., Huston, D.L., Peter, J.M., 2021. Toward an effective global green economy: the Critical Minerals Mapping Initiative (CMMI). SGA News 8, 1–5.
Kerrich, R.Bursnall, J.T. (Ed.), 1989. Geodynamic setting and hydraulic regimes: shear zone hosted mesothermal gold deposits. Mineralization and Shear Zones 6, 89–128.
Knox-Robinson, C.M., Wyborn, L.A.I., 1997. Towards a holistic exploration strategy: using geographic information systems as a tool to enhance exploration. Aust. J. Earth Sci. 44, 453–463.
Kolb, J., Dziggel, A., Bagas, L., 2015. Hypozonal lode gold deposits: a genetic concept based on a review of the New Consort, Renco, Hutti, Hira Buddini, Navachab, Nevoria and The Granites deposits. Precambrian Res. 262, 20–44.
Kolb, J., Meyer, M.F., 2002. Fluid inclusion record of the hypozonal orogenic Renco gold deposit (Zimbabwe) during the retrograde P–T evolution. Contrib. Mineral. Petrol. 143, 495–509.
Kolb, J., Rogers, A., Meyer, F.M., 2005a. Relative timing of deformation and two-stage gold mineralization at Hutti mine, Dharwar Craton, India. Miner. Depos. 40, 156–174.
Kolb, J., Sindern, S., Kisters, A.F.M., Meyer, F., Hoernes, S., Schneider, J., 2005b. Timing of Uralian orogenic gold mineralization at Kochkar in the evolution of the East Uralian granite-gneiss terrane. Miner. Depos. 40, 473–491.
Kontak, D.J., Smith, P.K., Kerrich, R., Williams, P.F., 1990. Integrated model for Meguma Group lode gold deposits, Nova Scotia, Canada. Geology 18, 238–242.
Korges, M., Weis, P., Andersen, C., 2020. The role of incremental magma chamber growth on ore formation in porphyry copper systems. Earth Planet. Sci. Lett. 552, 116584.
Kreuzer, O.P., Etheridge, M.A., Guj, P., McMahon, M.E., Holden, D.J., 2008. Linking mineral deposit models to quantitative risk analysis and decision-making in exploration. Econ. Geol. 103, 829–850.
Kwan, K., Müller, D., 2020. Mount Milligan alkalic porphyry Au–Cu deposit, British Columbia, Canada, and its AEM and AIP signatures: implications for mineral exploration in covered terrains. J. Appl. Geophys. 180, 104131.
LaFlamme, C., Jamieson, J.W., Fiorentini, M.L., Thebaud, N., Caruso, S., Selvaraja, V., 2018. Investigating sulfur pathways through the lithosphere by tracing mass independent fractionation of sulfur to the Lady Bountiful orogenic gold deposit, Yilgarn Craton. Gondwana Res. 58, 27–38.
Lang, J.R., Baker, T., Hart, C.J.R., Mortensen, J.K., 2000. An exploration model for intrusion-related gold systems. SEG Newsl. 40, 6–15.
Large, R.R., Danyushevsky, L.V., Hollit, C., Maslennikov, V., Meffre, S., Gilbert, S., Bull, S., Scott, R., Emsbo, P., Thomas, H., Foster, J., 2009. Gold and trace element zonation in pyrite using a laser imaging technique: implications for the timing of gold in orogenic and Carlin-style sediment- hosted deposits. Econ. Geol. 104, 635–668.
Lee, C.T.A., Leeman, W.P., Canil, D., Li, Z.X.A., 2005. Similar V/*Sc* systematic in MORB and arc basalts: implications for the oxygen fugacities of their mantle source regions. J. Petrol. 46, 2313–2336.
Lee, C.T.A., Luffi, P., Chin, E.J., Bouchet, R., Dasgupta, R., Morton, D.M., Le Roux, V., Yin, Q.Z., Jin, D., 2012. Copper systematics in arc magmas and implications for crust-mantle differentiation. Science 336, 64–68.
Lee, R.G., Dilles, J.H., Tosdal, R.M., Wooden, J.L., Mazdab, F.K., 2017. Magmatic evolution of granodiorite intrusions at the El Salvador porphyry copper deposit, Chile, based on trace element composition and U/Pb age of zircons. Econ. Geol. 112, 245–273.
Li, S.R., Santosh, M., 2017. Geodynamics of heterogeneous gold mineralization in the North China Craton and its relationship to lithospheric destruction. Gondwana Res. 50, 267–292.
Li, Y., Selby, D., Feely, M., Costanzo, A., Li, X.H., 2017. Fluid inclusion characteristics and molybdenite *Re*-Os geochronology of the Qulong porphyry Cu-Mo deposit, Tibet. Miner. Depos. 52, 137–158.
Li, N., Deng, J., Yang, L.Q., Groves, D.I., Liu, X., Dai, W.G., 2018. Constraints on depositional conditions and ore-fluid source for orogenic gold districts in the West Qinling Orogen, China: implications from sulfide assemblages and their trace-element geochemistry. Ore Geol. Rev. 102, 204–209.
Lin, S.F., Beakhouse, G.P., 2013. Synchronous vertical and horizontal tectonism at late stages of Archean cratonization and genesis of Hemlo gold deposit, Superior craton, Ontario, Canada. Geology 41, 359–362.
Loader, M.A., 2017. Mineral Indicators of Porphyry Cu Fertility. In: PhD Thesis. Imperial College London, p. 436 Unpubl..
Loader, M.A., Wilkinson, J.J., Armstrong, R.N., 2017. The effect of titanite crystallization on Eu and Ce anomalies in zircon and its implications for the assessment of porphyry Cu deposit fertility. Earth Planet. Sci. Lett. 472, 107–119.
Lopez Orrego, G.P. (.2007). The El Espino Iron-oxide copper gold district, Coastal Cordillera of north-central Chile. Unpubl. PhD, Colorado School of Mines, Golden, 150pp.
Loucks, R.R., 2014. Distinctive composition of copper-ore-forming magmas. Aust. J. Earth Sci. 61, 5–16.
Lowell, J.D., Guilbert, J.M., 1970. Lateral and vertical alteration-mineralization zoning in porphyry ore deposits. Econ. Geol. 65, 373–408.
Lowell, J.D., 1974. Regional characteristics of porphyry copper deposits of the Southwest. Econ. Geol. 69, 601–617.
Lu, Y.J., Loucks, R.R., Fiorentini, M.L., McCuaig, T.C., Evans, N.J., Yang, Z.M., Hou, Z.Q., Kirkland, C.L., Parra-Avila, L.A., Kobussen, A., 2016. In: Zircon Compositions as a Pathfinder for Porphyry Cu±Mo±Au Deposits, 19. Society of Economic Geologists Special Publication, pp. 329–347.
Maier, W.D., Groves, D.I., 2011. Temporal and spatial controls on the formation of magmatic PGE and Ni-Cu deposits. Miner. Depos. 46, 841–858.
Mair, J., Farmer, L., Groves, D., Hart, C., Goldfarb, R., 2011. Petrogenesis of mid-Cretaceous post-collisional magmatism at Scheelite Dome, central Yukon Territory, Canada—Evidence for a lithospheric mantle source. Econ. Geol. 106, 451–480.
Mao, J.W., Chen, Y.B., Chen, M.H., Pirajno, F., 2013. Major types and time–space distribution of Mesozoic ore deposits in South China and their geodynamic settings. Miner. Depos. 48, 267–294.
Matteini, M., Mazzuoli, R., Omarini, R., Cas, R., Maas, R., 2002. The geochemical variations of the upper Cenozoic volcanism along the Calama–Olacapato–El Toro transversal fault system in central Andes (24° S): petrogenetic and geodynamic implications. Tectonophysics 345, 211–227.
McCafferty, A.E., Phillips, J.D., Hofstra, A.H., Day, W.C., 2019. Critical architecture beneath the southern Midcontinent (USA) and controls on Mesoproterozoic iron-oxide mineralization from 3D geophysical models. Ore Geol. Rev. 111, 102966.
McCuaig, T.C., Beresford, S., Hronsky, J., 2010. Translating the mineral systems approach into an effective exploration targeting system. Ore Geol. Rev. 38, 128–138.
McCuaig, T.C., Hronsky, J.M.A., 2014. The mineral system concept: the key to exploration targeting. In: Proceedings of the SEG 2014: Building Exploration Capability for the 21st Century, pp. 153–175.
McInnes, B.I.A., Evans, N.J., Fu, F.Q., Garwin, S., 2005. Application of thermochronology to hydrothermal ore deposits. Rev. Mineral. Geochem. 58, 467–498.
Megill, R.E., 1988. Exploration Economics: Tulsa. PennWell, p. 238.
Meinert, L.D., Dipple, G.M., Nicolescu, S., 2005. World skarn deposits. In: Proceedings of the Economic Geology 100th Anniversary Volume, pp. 299–336.
Mercer, C.N., Reed, M.H., Mercer, C.M., 2015. Time scales of porphyry Cu deposit formation: insights from titanium diffusion in quartz. Econ. Geol. 110, 587–602.
Mpodozis, C., Cornejo, P., 2012. In: Cenozoic Tectonics and Porphyry Copper Systems of the Chilean Andes, 16. Economic Geology Special Publication, pp. 329–360.
Muir, T.L. (.1997). Precambrian geology of the Hemlo gold deposit area. *Ont. Geol. Sur.*, Report 289.
Müller, D., Franz, L., Herzig, P.M., Hunt, S., 2001. Potassic igneous rocks from the vicinity of epithermal gold mineralization, Lihir Island, Papua New Guinea. Lithos 57, 163–186.

Müller, D., Herzig, P.M., Scholten, J.C., Hunt, S., 2002. In: Ladolam Gold Deposit, Lihir Island, Papua New Guinea: Gold Mineralization Hosted by Alkaline Rocks, 9. Economic Geology Special Publication, pp. 367–382.
Müller, D., Groves, D.I., 2019. Potassic Igneous Rocks and Associated Gold-Copper Mineralization. Mineral Resource Reviews Springer, Cham, Switzerland, pp. 1–398.
Muntean, J.L., Cline, J.S., Simon, A.C., Longo, A.A., 2011. Magmatic–hydrothermal origin of Nevada's Carlin-type gold deposits. Nat. Geosci. 4, 122–127.
Murakami, H., Seo, J.K., Heinrich, C.A., 2009. The relation between Cu/Au ratio and formation depth of porphyry-style Cu–Au ± Mo deposits. Miner. Depos. 45, 11–21.
Nalpas, T., Dabard, M.P., Ruffet, G., Vernon, A., Mpodozis, C., Loi, A., Herail, G., 2008. Sedimentation and preservation of the Miocene Atacama Gravels in the Pedernales–Chañaral Area, Northern Chile: climatic or tectonic control? Tectonophysics 459, 161–173.
O'Hara, M.J., Mathews, R.E., 1981. Geochemical evolution in an advancing, periodically replenished, periodically tapped, continuously fractionated magma chamber. J. Geol. Soc. Lond. 138, 237–277.
O'Reilly, S.Y., Griffin, W.L., 2010. The continental lithosphere-asthenosphere boundary: can we sample it? Lithos 120, 1–13.
O'Reilly, S.Y., Griffin, W.L., 2013. Mantle metasomatism. In: Harlov, D.E., Austrheim, H. (Eds.), Metasomatism and the Chemical transformation of Rock: The Role of Fluids in Terrestrial and Extraterrestrial Processes. Springer Nature, pp. 471–533.
Oliver, N.H.S., Blenkinsop, T.G., Cleverley, J.S., Marshall, L.R., Ridd, P.J., 2006. Granite-related overpressure and release in the mid crust: fluidized breccias from the Cloncurry district, Australia. Geofluids 6, 346–358.
Olson, N.H., Dilles, J.H., Kent, A.J.R., Lang, J.R., 2017. Geochemistry of the Cretaceous Kaskanak batholith and genesis of the Pebble porphyry Cu-Au-Mo deposit, SW Alaska. Am. Mineral. 102, 1597–1621.
Parker, P., Bartlett, J., Hodges, K., Thompson, A., Standing, J.G., 2017. Nova-Bollinger Ni-Cu-Co sulfide deposit. In: Phillips, G.N. (Ed.), Australian Ore Deposits. Monograph 32. Australasian Institute of Mining and Metallurgy Melbourne, pp. 139–142.
Partington, G.A., 2017. Greenbushes, tin, tantalum, and lithium deposit. In: In Australian Ore Deposits, 32. Australian Institute of Mining and Metallurgy Monograph, pp. 153–157.
Peacock, S.M., Christensen, N.I., Bostock, M.G., Audet, P., 2011. High pore pressures and porosity at 35km depth in the Cascadia subduction zone. Geology 39, 471–474.
Perring, C.S., Groves, D.I., Ho, S.E., 1987. Constraints on the source of auriferous fluids for Archaean gold deposits. In: Ho, S.E., Groves, D.I. (Eds.), Recent Advances in Understanding Precambrian Gold Deposits, Publication 11. Geology Department and University Extension, University of Western Australia, pp. 287–306.
Phillips, G.N., Powell, R., 2010. Formation of gold deposits-a metamorphic devolatilization model. J. Metamorph. Geol. 28, 689–718.
Pitcairn, I.K., Teagle, D.A.H., Craw, D., Olivo, G.R., Kerrich, R., Brewer, T.S., 2006. Sources of metals and fluids in orogenic gold deposits: insights from the Otago and Alpine Schists, New Zealand. Econ. Geol. 101, 1525–1546.
Portela, B., Sepp, M.D., van Ruitenbeek, F.J.A., Hecker, C., 2021. Using hyperspectral imagery for identification of pyrophyllite-muscovite intergrowths and alunite in the shallow epithermal environment of the Yerington porphyry copper district. Ore Geol. Rev. 131, 104012.
Pour, A.B., Hashim, M., 2012. The application of ASTER remote sensing to porphyry copper and epithermal gold deposits. Ore Geol. Rev. 44, 1–9.
Prendergast, K., Clarke, G.W., Pearson, N.J., Harris, K., 2005. Genesis of pyrite-Au-As-Zn-Bi-Te zones associated with Cu-Au skarns: evidence from the Big Gossan and Wanagon gold deposits, Ertsberg District, Papua, Indonesia. Econ. Geol. 100, 1021–1050.
Profeta, L., Ducea, M.N., Chapman, J.B., Paterson, S.R., Gonzales, S.M., Kirsch, M., Petrescu, L., DeCelles, P.G., 2015. Quantifying crustal thickness over time in magmatic arcs. Sci. Rep. 5, 17786.
Radhakrishna, B.P., Curtis, L.C., 1999. Gold in India. Geological Society of India, Bangalore, p. 307.
Richards, J.P. (.1995). Alkalic-type epithermal gold deposits – a review. In: J. F. H., Thompson (Ed.), Magmas, Fluids and Ore Deposits. Mineralogical Association of Canada, Toronto, Vol. 23, 367–400.
Richards, J.P., 2009. Post-subduction porphyry Cu-Au and epithermal Au deposits: products of remelting of subduction-modified lithosphere. Geology 37, 247–250.
Ridley, J.R., Diamond, L.W., 2000. Fluid chemistry of orogenic lode gold deposits and implications for genetic models. Rev. Econ. Geol. 13, 141–162.
Robertson, K., Thiel, T., 2019. In: Detecting the Fingers of God: Optimising Magnetotelluric Survey Design for Mineral Exploration, 1. Australian Society of Exploration Geophysics Extended Abstracts, pp. 1–3.
Rock, N.M.S., Groves, D.I., Perring, C.S., Golding, S.D., 1989. Gold, lamprophyres, and porphyries: what does their association mean? Econ. Geol. Monogr. 6, 609–625.
Rosenbaum, J.M., Zindler, A., Rubenstone, J.L., 1996. Mantle fluids: evidence from fluid inclusions. Geochim. Cosmochim. Acta 60, 3229–3252.
Ryan, R.J., Smith, P.K., 1998. A review of the mesothermal gold districts of the Meguma Group, Nova Scotia Canada. Ore Geol. Rev. 13, 153–183.
Safonova, I.Y., Utsunomia, A., Kojima, S., Nakae, S., Tomurfogoo, O., Filippov, A.N., Koizumi, K., 2009. Pacific superplume-related oceanic basalts hosted by accretionary complex of Central Asia, Russian Far East, and Japan. Gondwana Res. 16, 587–608.
Salfity, J.A., 1985. Lineamentos transversales al rumbo andino en el noroeste argentino. IV Congreso Geológico Chileno, Actas 2. Asociación Geológica Argentina, Antofagasta, pp. 119–137.
Santosh, M., 2010. A synopsis of recent conceptual models on supercontinent tectonics in relation to mantle dynamics, life evolution and surface environment. J. Geodyn. 50, 116–133.
Sarma, D.S., Fletcher, I.R., Rasmussen, B., McNaughton, N.J., Mohan, M.R., Groves, D.I., 2011. Archaean gold mineralization synchronous with late cratonization of the Western Dharwar Craton, India: 2.52 Ga U-Pb ages of hydrothermal monazite and xenotime in gold deposits. Miner. Depos. 46, 273–288.
Saunders, J.E., Pearson, N.J., O'Reilly, S.Y., Griffin, W.L., 2018. Gold in the mantle: a global assessment of abundance and redistribution processes. Lithos 322, 376–391.
Schodde, R.C. (.2017). Long-term forecast of Australia's mineral production and revenue. The outlook for gold: 2017-2057. Special study commissioned by the Australian government and industry by MinEx Consulting, October 2017:89p
Seedorff, E., Dilles, J.H., Proffett, J.M.Jr., Einaudi, M.T., Zurcher, L., Stevast, W.J.A., Johnson, D.A., Barton, M.D., 2005. Porphyry deposits: characteristics and hypogene features. In: Proceedings of the Economic Geology 100th Anniversay Volume, pp. 251–298.
Seedorff, E., Barton, M.D., Stavast, W.J.A., Maher, D.J., 2008. Root zones of porphyry systems: extending the porphyry model to depth. Econ. Geol. 103, 939–956.
Selvaraja, V., Caruso, S., Fiorentini, M.L., LaFlamme, C., Bui, T.H., 2017. Atmospheric sulfur in the orogenic gold deposits of the Archean Yilgarn Craton, Australia. Geology 45, 691–695.
Seno, T., Kirby, S.H., 2014. Formation of plate boundaries: the role of mantle devolatilization. Earth Sci. Rev. 129, 85–99.
Sibson, R.H., 2004. Controls on maximum fluid overpressure defining conditions for mesozonal mineralization. J. Struct. Geol. 26, 1127–1136.
Sibson, R.H., 2013. Stress switching in subduction forearcs: implications for overpressure containment and strength cycling on megathrusts. Tectonophysics 600, 142–152.
Sillitoe, R.H., 1972. A plate-tectonic model for the origin of porphyry copper deposits. Econ. Geol. 67, 184–197.
Sillitoe, R.H., 1979. Some thoughts on gold-rich porphyry copper deposits. Miner. Depos. 14, 161–174.
Sillitoe, R.H., 1994. Erosion and collapse of volcanoes: causes of telescoping in intrusion-centered ore deposits. Geology 22, 945–948.
Sillitoe, R.H., 2000. Gold-rich porphyry deposits: descriptive and genetic models and their role in exploration and discovery. Soc. Econ. Geol. Rev. 13, 315–345.
Sillitoe, R.H., 2010. Porphyry copper systems. Econ. Geol. 105, 3–41.
Sillitoe, R.H., 2020. In: Gold Deposit Types: An Overview, 23. Society of Economic Geologists Special Publication, pp. 1–28.
Sillitoe, R.H., Hedenquist, J.W., 2003. In: Linkages Between Volcanic Settings, Ore-Fluid Compositions, and Epithermal Precious Metal Deposits, 10. Society of Economic Geologists Special Publication, pp. 315–346.
Sillitoe, R.H., Perello, J., 2005. Andean copper province: tectonomagmatic settings, deposit types, metallogeny, exploration, and discovery. In: Proceedings of the Economic Geology 100th Anniversary Volume, pp. 845–890.
Skirrow, R.G., Murr, J., Schoffield, A., Huston, D.L., van der Wielen, S., Czarnota, K., Coghlan, R., Highet, L.M., Connelly, D., Doublier, M., Duan, J., 2019. Mapping iron oxide Cu-Au (IOCG) mineral potential in Australia using a knowledge-driven mineral systems-based approach. Ore Geol. Rev. 113, 103011.
Spandler, C., Slezak, P.R., Nazari-Dehkordi, T., 2020. Tectonic significance of Australian rare earth element deposits. Earth Sci. Rev. 207, 103219.
Steadman, J.A., Large, R.R., Meffre, S., Bull, S.W., 2013. Age, origin, and significance of nodule sulfides in 2680 Ma carbonaceous black shale of the Eastern Goldfields Superterrane, Yilgarn craton, Western Australia. Precambrian Res. 230, 227–247.
Sun, W., Huang, R.F., Li, H., Hu, Y.B., Zhang, C.C., Sun, S.J., Zhang, L.P., Ding, X., Li, C.Y., Zartman, R.E., Ling, M.X., 2015. Porphyry deposits and oxidized magmas. Ore Geol. Rev. 65, 97–131.
Tatsumi, Y., Eggins, S., 1995. Subduction Zone Magmatism. Frontiers in Earth Sciences Blackwell Science, Boston, pp. 1–211.
Tomkins, A.G., 2010. Windows of metamorphic sulfur liberation in the crust: implications for gold deposit genesis. Geochim. Cosmochim. Acta 74, 3246–3259.
Tripp, G., 2014. How Neoarchean stratigraphy and structural geology determine the timing and controls of world-class greenstone gold camps in the Eastern Goldfields Province: key factors for gold exploration. Gold'14 Extended Abstracts. Aust. Inst. Geosci. Bull. 59, 124–128.
Turner, S.J., Reynolds, J., Hagemann, S.G., 2020. In: Boddington: An Enigmatic Giant Archean Gold-Copper (molybdenum-silver) Deposit in the Southwest Yilgarn Craton, Western Australia, 23. Society of Economic Geologists Special Publication, pp. 275–288.
Ulrich, T., Günther, D., Heinrich, C.A., 2001. The evolution of a porphyry Cu-Au deposit, based on LA-ICP-MS analysis of fluid inclusions: bajo de la Alumbrera, Argentina. Econ. Geol. 96, 1743–1774.
Urzua, F., 2009. Geology, Geochronology and Structural Evolution of La Escondida Copper District, Northern Chile. University of TasmaniaAustralia, Hobart, p. 486 Unpublished PhD Thesis.
Vasanthi, A., Santosh, M., 2021. Lithospheric architecture and geodynamics of the Archean Dharwar craton and surrounding terranes: new insights from satellite gravity investigation. Gondwana Res. 95, 14–28.
Waite, K.A., Keith, J.D., Christiansen, E.H., Whitney, J.A., Hattori, K., Tingey, G.D., Hook, C.J., 1997. Petrogenesis of the volcanic and intrusive rocks associated with the Bingham Canyon porphyry Cu-Au-Mo deposit, Utah. Econ. Geol. Guideb. 29, 69–90.

Wang, Q.F., Groves, D.I., 2018. Carlin-style gold deposits, Youjiang Basin, China: tectono-thermal and structural analogues of the Carlin-type gold deposits, Nevada, USA. Miner. Depos. 53, 909–918.
Wang, Q.F., Groves, D.I., Deng, J., Li, H., Yang, L., Dong, C., 2020a. Evolution of the Miocene Ailaoshan gold deposits, southeastern Tibet, during a complex tectonic history of lithosphere-crust interaction. Miner. Depos. 55, 1085–1104.
Wang, Q.F., Zhao, H.S., Groves, D.I., Deng, J., Zhang, Q.Z., Xue, S.C., 2020b. The Jurassic Danba hypozonal orogenic gold deposit, western China: indirect derivation from fertile mantle lithosphere metasomatized during Neoproterozoic subduction. Miner. Depos. 55, 309–324.
Wang, R., Zhu, D.C., Wang, Q., Hou, Z.Q., Yang, Z.M., Zhao, Z.D., Mo, X.X., 2020c. Porphyry mineralization in the Tethyan orogen. Sci. China Earth Sci. 62, 2042–2067.
Wang, Z.C., Cheng, H., Zong, K.Q., Geng, X.L., Liu, Y.S., Yang, J.H., Wu, F.Y., Becker, H., Foley, S., Wang, C.Y., 2020d. Metasomatized lithospheric mantle for Mesozoic giant gold deposits in the North China craton. Geology 48, 169–173.
Wang, Y., Zhou, L.Y., Luo, Z.H., 2017. Kinematics and timing of continental block deformation from margins to interiors. Tera Nova 29, 253–263.
Waters, L.E., Cottrell, E., Coombs, M.L., Kelley, K.A., 2021. Generation of calc-alkaline magmas during crystallization at high oxygen fugacity: an experimental and petrologic study of tephras from Buldir Volcano, western Aleutian Arc, Alaska, USA. J. Petrol. 62. doi:10.1093/petrology/egaa104.
White, A.J.R., Waters, D.J., Robb, L.J., 2015. Exhumation-driven devolatilization as a fluid source for orogenic gold mineralization at the Damang deposit, Ghana. Econ. Geol. 110, 1009–1026.
Wilkinson, J.J., 2013. Triggers for the formation of porphyry ore deposits in magmatic arcs. Nat. Geosci. 6, 917–925.
Wilkinson, J.J., Baker, M.J., Cooke, D.R., Wilkinson, C.C., 2020. Exploration targeting in porphyry Cu systems using propylitic mineral chemistry: a case study of the El Teniente deposit, Chile. Econ. Geol. 115, 771–791.
Williams, H.M., Prytulak, J., Woodhead, J.D., Kelley, K.A., Brounce, M., Plank, T., 2018. Interplay of crystal fractionation, sulfide saturation and oxygen fugacity on the iron isotope composition of arc lavas: an example from the Marianas. Geochim. Cosmochim. Acta 226, 224–243.
Witt, W.K., Ford, A., Hanrahan, B., Mamuse, A., 2013. Regional-scale targeting for gold in the yilgarn craton: part 1 of the yilgarn gold exploration targeting Atlas. Geol. Surv. Western Aust. Rep. 125, 130.
Wyborn, L.A.I., Heinrich, C.A., Jaques, A.L., 1994. Australian Proterozoic mineral systems: essential ingredients and mappable criteria. In: Proceedings of the Australasian Institute of Mining and Metallurgy Annual Conference, Melbourne, pp. 109–115.
Wyman, D.A., Cassidy, K.F., Hollings, P., 2016. Orogenic gold and the mineral systems approach: resolving fact, fiction and fantasy. Ore Geol. Rev. 78, 322–335.
Wyman, D.A., Kerrich, R., 2002. Formation of Archean continental lithospheric roots: the role of mantle plumes. Geology 30, 543–546.
Wyman, D.A., O'Neill, C.O., Ayer, J.A., 2008. In: Evidence for Modern-Style Subduction to 3.1Ga: a Plateau-Adakite-gold (diamond) Association, 440. Geological Society of America Special Publication, pp. 129–148.
Yang, C.X., Santosh, M., 2020. Ancient deep roots for Mesozoic world-class gold deposits in the north China craton: an integrated genetic perspective. Geosci. Front. 11, 203–214.
Yang, K.F., Fan, H.R., Pirajno, F., Li, X., 2019. The Bayan Obo (China) giant REE accumulation conundrum elucidated by intense magmatic differentiation of carbonatite. Geology 47, 1198–1202.
Yang, L.Q., Deng, J., Wang, Z.L., Guo, L.N., Li, R.H., Groves, D.I., Danyushevsky, L.V., Zhang, C., Zheng, X.L., Zhao, H., 2016. Relationships between gold and pyrite at the Xincheng gold deposit, Jiaodong Peninsula, China: implications for gold source and deposition in a brittle epizonal environment. Econ. Geol. 111, 105–126.
Yang, L.Q., Deng, J., Groves, D.I., He, W.Y., Li, N., Zhang, L., Zhang, R.R., 2021. China's Anomalously Rich Mineral Endowment: The Critical Role of 'Metallogenic Factories' on Craton Margins. Geological Society of America Bulletin (submitted).
Zhang, L., Weinberg, R.F., Yang, L.Q., Groves, D.I., Sai, S.X., Matchan, E., Phillips, D., Kohn, B.P., Miggins, D.P., Liu, Y., Deng, J., 2020a. Mesozoic orogenic gold mineralization in the Jiaodong Peninsula, China: a focused event at ca. 120 Ma during cooling of pre-gold granite intrusions. Econ. Geol. 115, 415–441.
Zhang, L., Groves, D.I., Yang, L.Q., Sun, S.C., Weinberg, R.F., Wang, J.X., Wu, S.G., Gao, L., Yuan, L.L., Li, R.H., 2020b. Utilization of pre-existing competent and barren quartz veins as hosts to later orogenic gold ores at the Huangjindong gold deposit, Jiangnan Orogen, southern China. Miner. Depos. 55, 363–380.
Zhang, R.Z., Zhang, D.H., Wu, M.Q., Hou, H.G., Li, X.L., 2021. Genesis of the Shiyaogou porphyry Mo deposit at East Qinling, China: evidence from geochronological, fluid inclusion, geochemical whole-rock and isotope studies. Ore Geol. Rev. 136, 104263.
Zhao, H.S., Wang, Q.F., Groves, D.I., Deng, J., 2019. A rare Phanerozoic amphibolite-hosted gold deposit at Danba, Yangtze Craton, China: significance to fluid and metal sources for orogenic gold systems. Miner. Depos. 54, 133–152.
Zhong, S., Feng, C., Seltmann, R., Dai, Z., 2018. Geochemical contrasts between late Triassic ore-bearing and barren intrusions in the Weibao Cu-Pb-Zn deposit, east Kunlun Mountains, NW China: constraints from accessory minerals (zircon and apatite). Miner. Depos. 53, 855–870.

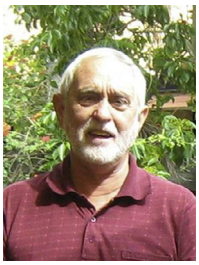

David Groves is Emeritus Professor in the centre for Exploration Targeting at the University of Western Australia (UWA) and Visiting Professor at the China University of Geosciences Beijing. Educated at Varndean Grammar School in Brighton, UK, and Hobart High School, Tasmania. BSc Honours (First Class) and PhD from the University of Tasmania, Honorary DSc from UWA, Member Australian Academy of Science. Former Director of Key centre for Strategic Mineral Deposits and centre for Global Metallogeny at UWA. Supervised over 250 BSc Honours, MSc and PhD students. Published approximately 500 papers and book chapters. Former President of Geological Society of Australia, SEG and SGA. Awarded 11 Research Medals including Gold Medals of SEG and SGA and the Geological Association of Canada Medal, plus other medals from Australia, South Africa, and UK. Currently Consultant through Orebusters Pty Ltd. to the mineral exploration industry and brokers and investors in Canada with exploration properties in Africa, Australia, Kazakhstan, and Quebec, Canada. Most recently a novelist The Digital Apocalypse, The Plagues' Protocol, King Solomon's Gold, Lasseter's Legendary Lost Reef, and Destiny on Magic White Mountain (in English and Mandarin).

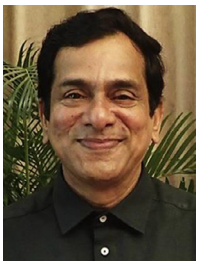

M. Santosh is Professor at the China University of Geosciences Beijing (CUGB), Specially Appointed Foreign Expert of China, Professor at the University of Adelaide, Australia and Emeritus Professor at the Faculty of Science, Kochi University, Japan. PhD (Cochin University of Science and Technology, India), D.Sc. (Osaka City University, Japan) and D.Sc. (University of Pretoria, South Africa). He is the Founding Editor of Gondwana Research as well as the founding Secretary General of the International Association for Gondwana Research. Research fields include petrology, fluid inclusions, geochemistry, geochronology, metallogeny and supercontinent tectonics. Published over 800 research papers, edited several memoir volumes and journal special issues, and co-author of the book 'Continents and Supercontinents' (Oxford University Press, 2004). Recipient of National Mineral Award, Outstanding Geologist Award, Thomson Reuters 2012 Research Front Award, Thomson Reuters High Cited Researcher 2014, 2015, 2016, and 2017.

Daniel Müller is a Consulting Geologist advising mining and exploration companies in target generation and on the prospect scale, based in Santiago de Chile. He graduated with a MSc in Geology and Mineralogy at the Johannes Gutenberg University Mainz, Germany, after serving for 3 years as First Lieutenant at German Air Force. He obtained his PhD at the Key centre for Strategic Mineral Deposits, University of Western Australia, Perth, Australia, and completed his Habilitations Degree at the Institute for Mineralogy, TU Bergakademie Freiberg, Germany. He is an experienced geologist with >27 years exploring for base- and precious-metal deposits with international mining companies in southern Africa, Asia, Australia, Europe, North and South America, and the Middle East. His exploration teams discovered additional resources of 200,000 ounces of gold both at Kanowna Belle Gold Mine, Australia, and at the Jabal Shayban Gold Project, Kingdom of Saudi Arabia, respectively. Daniel published more than 15 research papers and a textbook on high-K magmatism and hydrothermal gold-copper mineralization in five editions with Springer. He has been the recipient of numerous Scholarships as well as the Hesperian Press Postgraduate Award (1992) and the Western Mining Postgraduate Award (1993). Daniel is also a member of the Editorial Board of Ore Geology Reviews.

Liang Zhang is a Lecturer at CUGB. He obtained a B.Eng. (2011) from Hebei GEO University, was a Visiting Ph.D. student (2015) at Monash University, and received his Ph.D. from CUGB (2016). He has published more than 30 research papers as either first or co-author. He has been the recipient of Scientific and Technological Progress Awards (First prize, China Gold Association, 2021; First prize, Ministry of Education, China, 2014; Second prize, Shandong Province, China, 2014).

Jun Deng is a professor at the CUGB. He received his B.Sc. (1981) and M.Sc. (1989) degrees from the China University of Geosciences, Wuhan (CUGW), and Ph.D. (1992) from Chinese Academy of Geological Sciences. In the last 30 years, he has devoted himself to the genesis and resource prospects of gold deposits in Jiaodong. Since 2009, he has organized two National Key Basic Research Development Programs as chief scientist funded by Ministry of Sciences and Technology, China. These two programs contribute to the topic of "Accretionary and continent-collisional orogenesis and the associated mineralization in Tethyan regime, SW China."

Li-Qiang Yang is a professor at the CUGB. He received his B.Sc. degree (1996) from the CUGW, M.Sc. degree (1999) from the CUGB, and Ph.D. degree (2002) from Institute of Geology and Geophysics, Chinese Academy of Sciences. He was a visiting scholar at Denver centre, US Geological Survey (2009), Monash University (2015), and the University of Tasmania (2018). He works on the genesis and resource prospects of gold, copper and molybdenum deposits in Jiaodong, eastern China, and Sanjiang Tethyan domain, southwestern China. The main goal of his research is to understand the mechanism of formation of giant deposits and to apply genetic models to exploration.

Qing-Fei Wang is a professor at CUGB. He received a B.Sc. degree in 2000 from CUGW and a Ph.D. degree in 2005 from CUGB. He was a visiting scholar at Indiana University Bloomington, USA, in 2012. His current research focus is regional metallogeny in convergent tectonic settings, such as the Tethyan orogenic belts in Yunnan and Tibet, western China. The ultimate goal of his research is to develop geologic or genetic models that can be used for mineral exploration at both regional and deposit scales.